Chair of Petroleum and Geothermal Energy Recovery

Master's Thesis

Design of a Heat Exchanger for the Pump Test Facility

Maha Hasni, BSc

May 2021

MONTANUNIVERSITÄT LEOBEN
www.unileoben.ac.at

AFFIDAVIT

I declare on oath that I wrote this thesis independently, did not use other than the specified sources and aids, and did not otherwise use any unauthorized aids.

I declare that I have read, understood, and complied with the guidelines of the senate of the Montanuniversität Leoben for "Good Scientific Practice".

Furthermore, I declare that the electronic and printed version of the submitted thesis are identical, both, formally and with regard to content.

Date 25.05.2021

Signature Author
Maha Hasni

EIDESSTATTLICHE ERKLÄRUNG

Ich erkläre an Eid statt, dass ich die vorliegende Masterarbeit selbständig und ohne fremde Hilfe verfasst, andere als die angegebenen Quellen und Hilfsmittel nicht benutzt und die den benutzten Quellen wörtlich und inhaltlich entnommenen Stellen als solche erkenntlich gemacht habe.

Leoben, 18/05/2021
Maha Hasni

AFFIDAVIT

I hereby declare that the content of this work is my own composition and has not been submitted previously for any higher degree. All extracts have been distinguished using quoted references and all information sources have been acknowledged.

Leoben, 18/05/2021
Maha Hasni

Danksagung / Acknowledgement

I would like to thank my family for their endless support.

I would also like to acknowledge the time and effort put by my advisors into this work.

Kurzfassung

Wärmetauscher sind zweifelsfrei ein Grundstein in der fortschrittlichen und technischen Industrie, wobei sie eine bedeutende Vielzahl an Anwendungen aufweisen.
Darüber hinaus sind diese Vorrichtungen nicht nur im Alltag und für den häuslichen Gebrauch unverzichtbar, sondern spielen auch für energieeffiziente Praktiken eine wesentliche Rolle.

Die Pumpentestanlage unserer Universität erfordert einen Wärmetauscher, der für den ordnungsgemäßen Gebrauch im Pumpenlabor unabdingbar ist. Dafür wurde basierend auf spezifische Betriebszustände ein detaillierter Entwurf des Wärmetauschers entwickelt mit dem Ziel, die gewünschte Wärmeübertragung zu erlangen und einen gewissen Grad an Energieeffizienz zu erreichen.

Daraufhin wird eine thermodynamische Entwurfsmethode gekoppelt mit einem Mehrphasenmodell untersucht, das mit der Software OLGA simuliert wurde.
Abschließend werden beide Ergebnisse verglichen und übereingestimmt, um die optimalen Arbeitsbedingungen des konstruierten Wärmetauschers ermitteln zu können.

Abstract

It is certain that heat exchangers are a cornerstone in the modern industrial and technological scenery, as they mark their presence in a wide variety of applications.
As a matter of fact, not only are they indispensable in day-to-day life and in domestic environments, but they also come across as crucial for energy efficient practices in the industry.

Like so, the pump test facility in our university requires a heat exchanger which is needed for operations to be carried out properly at the pump lab. A detailed design of this heat exchanger is conducted based on specific operating conditions, in the goal of reaching the desired heat transfer and attaining a level of energy efficiency.

Thereupon, a thermodynamic design method is explored, paired with a multiphase model simulated using the software OLGA.
Finally, results of both tools are compared and matched to conclude optimum working conditions for the designed heat exchanger.

Table of Content

Page

1 INTRODUCTION 1

1.1 Background 1

1.2 Statement of problem 1

1.3 Objectives 1

2 FUNDAMENTALS 3

2.1 Classification 3

3 LITERATURE REVIEW: HEAT EXCHANGER APPLICATIONS IN LABORATORIES AND IN THE INDUSTRY 8

3.1 Introduction 8

3.2 Applications of heat exchangers 8

4 HEAT EXCHANGER DESIGN 17

4.1 Introduction to the ESP test stand 17

4.2 Data and Primary Estimations 17

4.3 Design Calculations 20

5 SIMULATION 32

5.1 Workflow 32

5.2 Modelling 32

5.3 Adjustments to real lab conditions: 43

6 RESULT COMPARISON 46

6.1 Comparing e-NTU to OLGA 46

6.2 Comparing testing Facility to OLGA 48

6.3 Comparing e-NTU method to testing facility 53

6.4 Interpretations 55

7 SUMMARY AND RECOMMENDATIONS 57

REFERENCES 58

LIST OF TABLES 60

LIST OF FIGURES 61

ABBREVIATIONS 63

NOMENCLATURE **64**

APPENDIX **66**

Results of the OLGA simulation under an insulated system 66

1 Introduction

1.1 Background

Thermodynamics, being one of the largest cornerstones of physics, also happens to be among the most important fields of interest for engineers. It is a very important sector lying underneath the explanation of natural phenomena as well as solving engineering-related problems.

That said, heat exchangers are a product of this domain. They present themselves as one of the most common devices used in all areas of engineering be it directly related to thermodynamics, or as a tool to solve secondary problems occurring within a certain installation during its operating time.

They are basically used to transfer heat between 2 fluids all the while keeping them separated. That is why their use is widespread and handy in many applications ranging between cooling and heating. [6]

In fact, some engineering tasks revolve around the heat exchanger as the main, and sometimes the only, component of the system. Examples of that would be refrigeration units and domestic heating equipment such as radiators. Meanwhile in many other cases, heat exchangers are introduced into complex systems as a transition step, or to prepare a certain product to be processed under specific conditions. An example of that is condensing units, heaters or boilers within refineries and processing facilities. [6]

1.2 Statement of problem

This research aims to come up with a heat exchanger design, enabling the university to cool hot water in the pump testing lab, and maintaining it at a constant temperature. For this purpose, the following steps to be conducted are explained below.

The work packages constituting this project can be carried out through three major parts. So, for starters, it is primordial to introduce the problematic of the topic as the foundation of the study.

Answering the questions: "Why do we need this heat exchanger?" and "Which problems are we trying to solve?" is essentially the driving force for this project. Consequently, given several primary data, we can make some early assumption as to what the end-product should look like, its basic characteristics and whether it is capable to meet the desired end-result. However, the resulting hypotheses can be altered further in the project since they are only based on assumptions.

1.3 Objectives

The objective of this research is to apply all acquired knowledge about heat exchangers and their range of application in order to design a proper heat exchanger of our own. This latter

will be addressed to solve a heat transfer issue at the pump testing facility at Montanüniversität Leoben. So, by the end of this project, a basic design of the desired heat exchanger will be up for manufacture.

The first step would then be to design the heat exchanger using basic thermodynamic calculations, while keeping in mind its specific environment. A couple of methods are available for designing heat exchangers. The choice depends solely on the available initial conditions and data within our reach.

After that, it is possible to create an OLGA model describing the fluid flow of the heat exchanger. The focal purpose of this model is to simulate the same conditions from a different perspective and to compare results of the hand calculations made in the previous step with those of the OLGA simulation. This creates room for additional interpretations, more accuracy and a means to improve the overall functioning of the design.

2 Fundamentals

Heat exchangers are one of the most common types of machinery found in many industries. They are very practical since they can reach efficient results with very simple designs, and highly versatile as they can be used in a large variety of tasks.

A heat exchanger's biggest feature is probably its ability to perform a heat transfer between two fluids without having to mix them. The fluids can be both liquids, a combination of a liquid and a gas, or even a solid and fluid. [12]

And since they are needed in multiple applications, they can vary in type and size, depending on the end goal they are meant to achieve.

Heat exchangers can then be classified according to their construction type, their flow arrangement, their size and to their type of heat transfer. [12]

2.1 Classification

2.1.1 According to construction type

Through the style of construction, the following types of heat exchangers can be distinguished:

- Shell and tube heat exchangers: thanks to their flexibility and to their robust design, they are the most common type of heat exchanger. As illustrated in figure 1 below, a bundle of pipes contained in a cylinder housing are its prime components. The cylinder is the shell, and the bundle of pipes is referred to as the tube. [13]

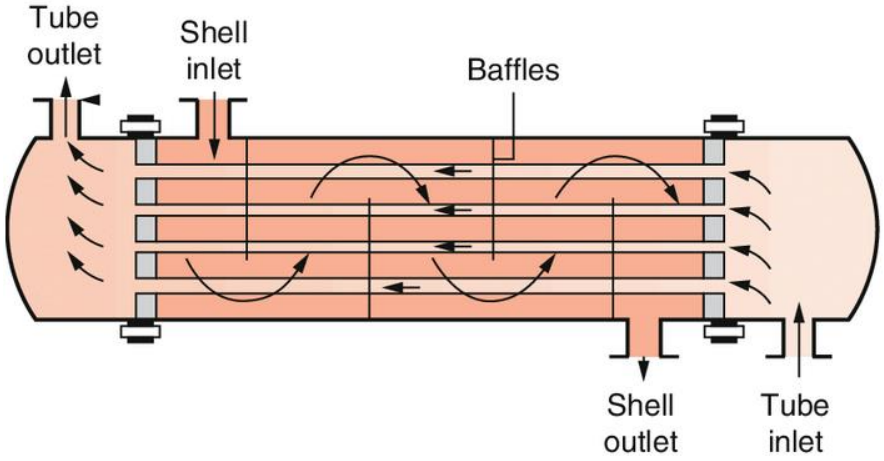

Figure 1: Schematic of a shell-and -tube HX [24]

- Double-pipe heat exchangers: As seen in figure 2, they consist of a configuration similar to that of the shell and tube heat exchanger. The difference is, for the former, the outer fluid flows in the shell, while for the latter, it circulates in the annular space separating two concentric pipes. [12]

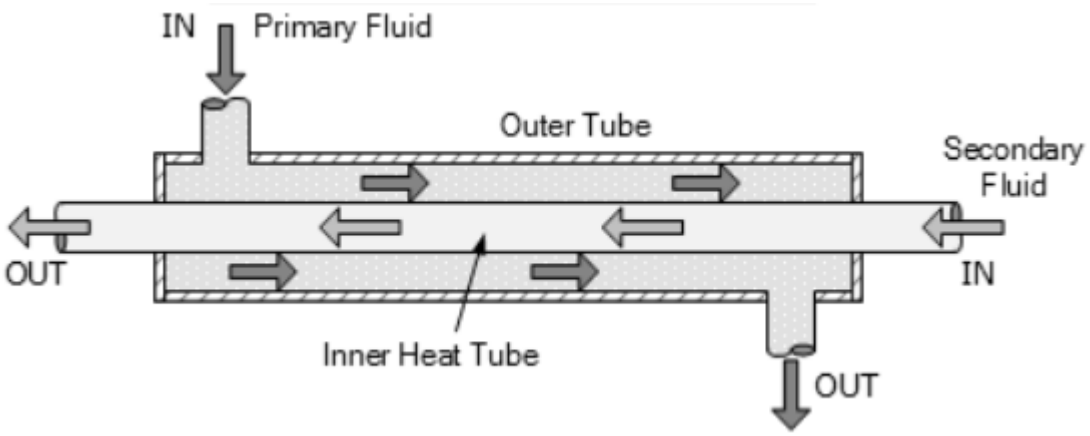

Figure 2: Schematic of a double-pipe HX [25]

- Finned-tube heat exchangers: It is possible to distinguish different types of finning for these heat exchangers like individual fins, longitudinal fins and flat external fins. Although the type of finning can vary widely, the common purpose for this type of construction is to increase the area of contact between the fluid and the wall, and therefore the surface area of heat transfer. [13]

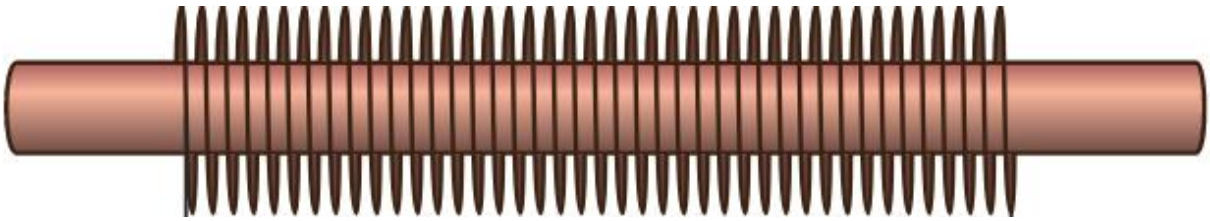

Figure 3: Schematic of a finned-tube HX [26]

- Plate heat exchangers: It is an innovative type of heat exchanger characterized by a very high heat transfer efficiency. This is ensured by its configuration of plates in series which allow the flow of hot and cold fluids in alternance. Although plate heat exchangers have limited pressure and temperature tolerance, they are widely praised for their flexibility, compactness and low maintenance with regards to cleaning and inspection. (See figure 6). [1]

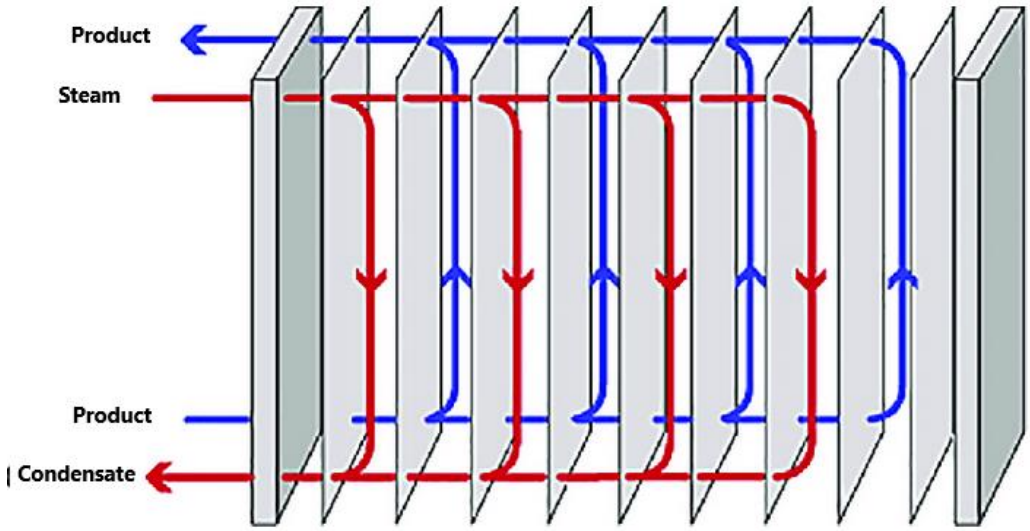

Figure 4: Schematic of a plate HX [28]

2.1.2 According to flow arrangement

The flow arrangement designates the flow direction of both fluids in relation to each other inside the heat exchanger. Accordingly, we can distinguish four types of flow arrangements:

- Parallel-flow heat exchangers: in this type of arrangement, the hot fluid and the cold fluid are flowing parallel to each other, meaning that their inlets are on the same side of the heat exchanger. This arrangement is not of high efficiency and is usually very prone to thermal stresses at the wall level, since both fluids enter with a big temperature difference. [1][13]
- Counter-flow heat exchangers: for this type of arrangement, hot fluids and cold fluids flow in opposite directions to each other, meaning that they enter the heat exchanger from opposite sides. This arrangement is very efficient in terms of heat transfer. [1]
  Both arrangements are shown in figure 4 below.

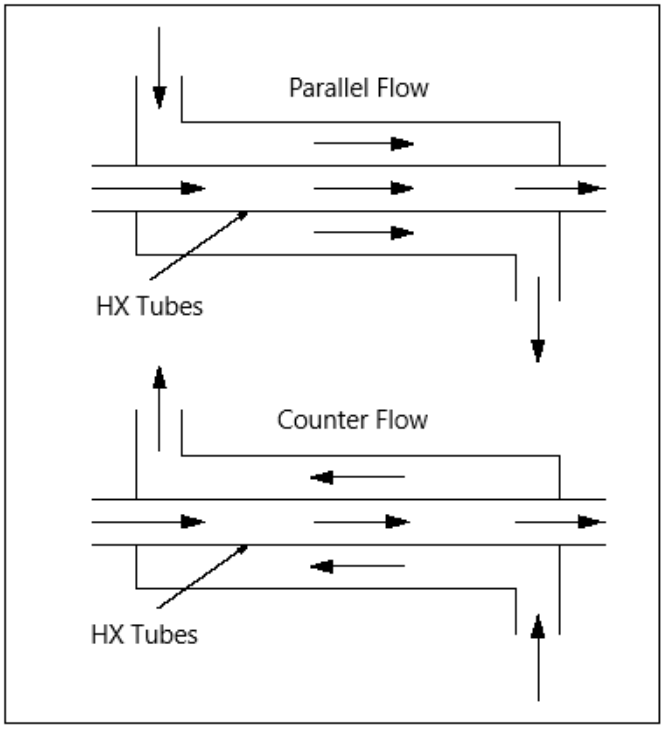

Figure 5: Schematic of parallel flow and counter flow arrangements [27]

- Crossflow heat exchangers: in this type of arrangement, both fluid directions are perpendicular to each other. The efficiency of this type of arrangement falls somewhere between those of the parallel-flow and counter-flow arrangements. [13]
  A typical scheme of the crossflow arrangement is presented in figure 5 below.

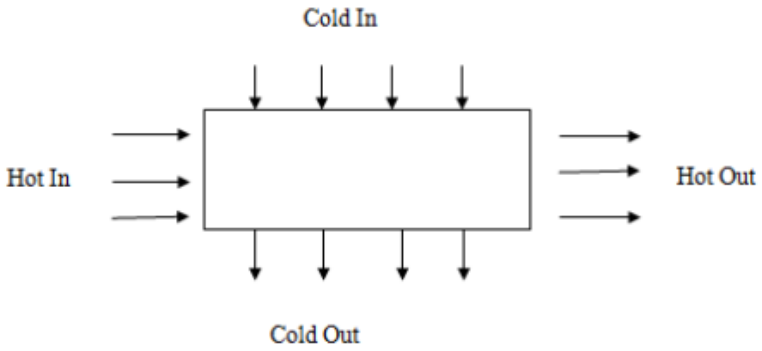

Figure 6: Schematic of a crossflow arrangement [27]

2.1.3 According to the type of heat transfer

There are three possible mechanisms of heat transfer that can occur within a heat exchanger, either individually or in combination:

- Single-phase convection, which can be either forced or free.
- Double-phase convection such as condensation or evaporation by forced or free convection.
- A combination of convection and radiation. [13]

2.1.4 According to size

A new generation of heat exchangers are compact heat exchangers. They are very handy especially when there are size and weight restrictions to the design. This type of heat exchanger is very efficient as it is characterized by a large surface area of the wall separating both fluids all while having low values of fluid flow resistance. This is expressed through their area density β, which is the ratio of the heat transfer surface area to their volume. For compact heat exchangers, this parameter is estimated by over 700 m^2/m^3. [1]

2.1.5 According to direct or indirect heat transfer

Heat transfer between fluids in a heat exchanger can occur either directly or indirectly. This usually means that both fluids are either flowing intermittently through the same flow path or are separated by a solid wall. On this basis, we can recognize two types of heat exchangers:

- Recuperators: are heat exchangers composed of a solid wall separating the fluids and where the heat transfer is done via convection and conduction: the former via fluids and the latter through the wall. This is the case of most heat exchangers mentioned before. [13]
- Regenerators: contrary to recuperators, regenerators do not offer a physical barrier separating both fluids. In fact, heat transfer between fluids is ensured indirectly by their alternate passage through the same flow paths. As a matter of fact, heat is stored in te matrix, and from there transferred to the fluid flowing by. The matrix can be fixed or rotating as exhibited in figure 7. Meanwhile, the drawback of regenerators is their high susceptibility to stress failures originating from constant alternation of different temperatures. In addition, the purity of the fluids is compromised since they share a single flow path. [13]

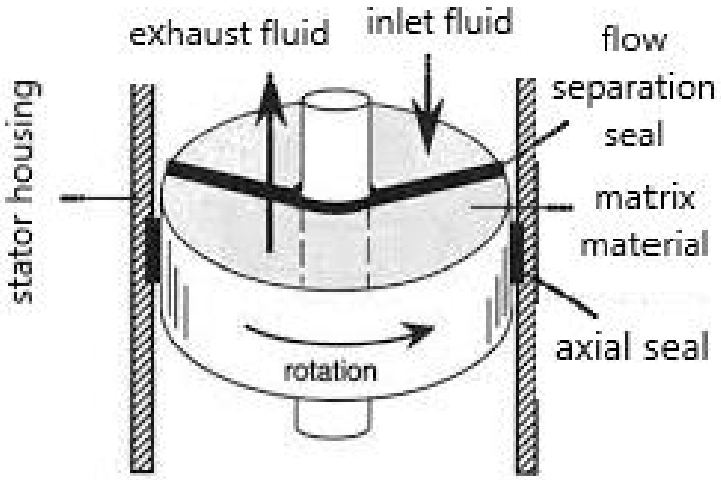

Figure 7: Schematic of a regenerator HX [29]

3 Literature Review: Heat exchanger applications in laboratories and in the industry

3.1 Introduction

The need for heat exchangers exceeds the industries and laboratories to englobe also everyday use within households. For that matter, they are among the most sought-after devices. Their function relies mainly on basic thermodynamics ensuring to bring one or more fluids to a desired temperature.

The role of a heat exchanger can be in essence its ability to transfer heat between two fluids, at different temperatures, while maintaining them separated. This certainly differentiates them from heat chambers that allow an exchange of heat by mixing both fluids together. Thus, heat transfer from the warmer fluid to the cooler one in a heat exchanger is assured by convection through the fluid and conduction through a solid wall. This is direct heat transfer for the case of heat exchangers. [1] [2]

The need for heat transfer is a cornerstone in so many applications varying from heating, cooling, boiling to condensing or even quality control by maintaining the temperature of a fluid at a constant threshold for example. Although the most trivial purposes of heat exchangers are those of day-to-day use in households, such as domestic space heating, air conditioning and refrigeration, they are a pillar in most laboratories and energy facilities as well.

That is why the presence of heat exchangers usually alongside other machinery is very common. In fact, they are extremely omnipresent in technical environments and within complex industrial networks where they serve as regulators for temperatures either to preserve handled products and maintain their quality, or to prepare them for certain processes. [7]

3.2 Applications of heat exchangers

3.2.1 In the petrochemical industry

3.2.1.1 In the Chemical industry

In general terms, there is a big demand for heat exchangers in any chemical-related activity such as process plants and laboratories. The need stems from the necessity to control temperatures of fluid streams; cold ones are to be heated, and vice versa.

Among the multiple reactions requiring heat transfer in the chemical industry, the most famous are probably distillation, stripping, absorption and evaporation. In the next segment, a description of the absorption and evaporation process is laid out. [8]

The process of absorption and evaporation is evidently a pillar in chemical engineering, and very common especially nowadays when our awareness of the environmental footprint is higher than ever.
In fact, one of its drivers is meeting environmental impact regulations related to chemical activities, and the second being minimum usage of solvent when recovering organic

components that are particularly volatile. This makes it not only an economically wise choice, but also environmentally conscious. [3]
A simple archetype of the absorption and evaporation process is illustrated in the figure below.

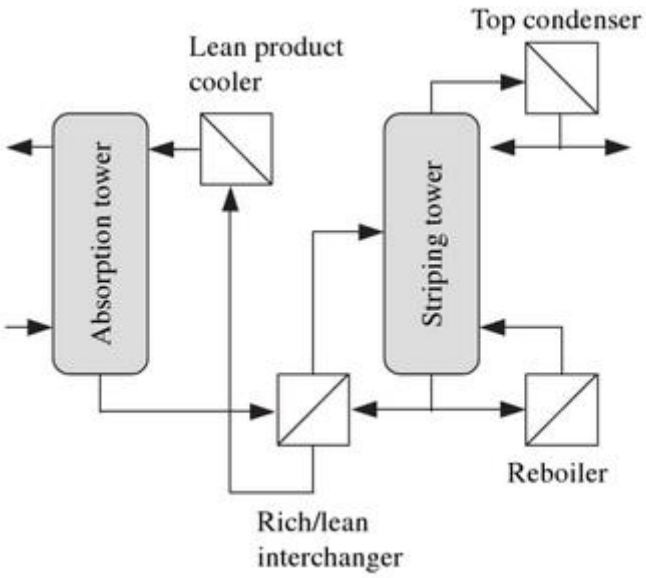

Figure 8: Absorption/evaporation flowchart [3]

This design is composed of two main stations: the absorption tower and the stripping tower.
The goal is to ensure that the lean absorption product coming from the interchanger is thoroughly cooled before entering the absorption tower. Simultaneously, after leaving the interchanger, the rich stripping medium should be preheated prior to entering the stripping tower.

For this process, engineers usually have recourse to plate or compact heat exchangers since they offer maximum heat recovery all the while using minimal external services dedicated to heating and cooling. [3]

3.2.1.2 In the oil and gas industry

The oil and gas industry are often labelled as the petrochemical industry since the use of heat exchangers in the oil and gas domain is mainly at surface level and has to do with product refining and storage. Consequently, this chapter is a particular case of the chemical industry, as the same concepts and principles apply, but the product is in fact a hydrocarbon.

As previously mentioned, heat transfer is required in many processes of the petrochemical chain and comes with a three-fold objective: firstly, to make sure that operations are being carried out under safe conditions, also to preserve the quality of the product and lastly to improve its storage for further use.

One of the many petrochemical processes is the cryogenic technology which is a very famous method used in the industry. It is identified as the ensemble of techniques and tools used to keep fluids below 120 degrees K° which is referred to as the cryogenic level. This facilitates the process of storage and transportation in large quantities of gases in a dense

liquid form rather than pressurized. Its most famous practice is related to the storage and shipping of natural gas. [7]

However, during the chemical process, cryogenic fluids are used in the gaseous form, thus require to be heated. The heating and vaporizing system of cryogenic liquids is depicted in the following figure.

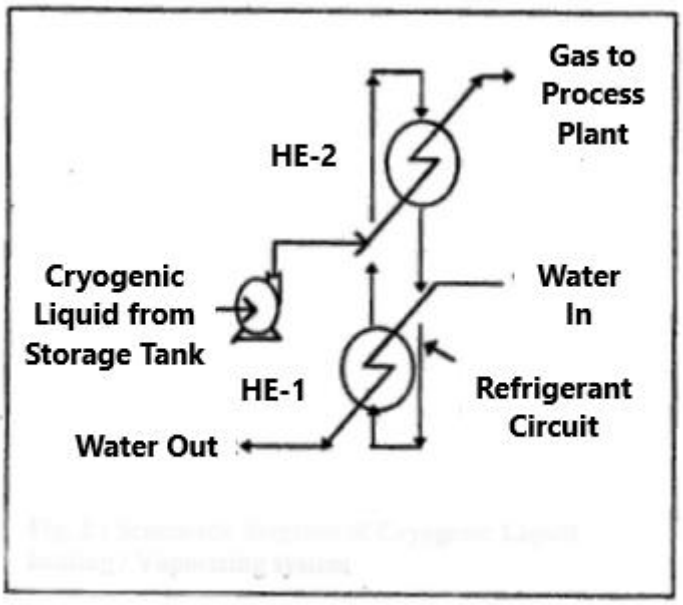

Figure 9: Petrochemical process of heating cryogenic fluids [7]

This system for example is comprised of two separate heat exchangers that provide different functions. In the lower compartment of the diagram, the first heat transfer in this procedure takes place at the first heat exchanger HE-1. Water is introduced into the system at high temperatures in order to evaporate the refrigerant. This latter, being an intermediate product in the process, has extremely low freezing temperatures, which requires that the water enters at very high temperatures.

The refrigerant, leaving the first heat exchanger, is vaporized at this point, and is introduced into a second heat exchanger HE-2. Here, the vaporized refrigerant serves as a heat agent, contributing in turn to the vaporization of the liquid cryogenic fluid. As a result of this interaction, the refrigerant is condensed again, and re-circulated in the cycle. Meanwhile, the cryogenic gas is ready to be used in the process plant. [7]

Shell and tube heat exchangers are commonly chosen in the process described above. That is due to their flexibility, reliability when dealing with high pressures and their relatively large heat transfer surface area in a small volume. Such a configuration ensures no contact between the water and the refrigerant during the first heat transfer process. In fact, putting them in contact may engender the freezing of the water, and this leads to physical damages affecting the heat exchanger. Moreover, recirculating the refrigerant in the system comes across as a very significant energy saving method. [7]

3.2.2 In the mechanical industry

It is undeniable that our need for transport, whether it involves us moving from one point to another or the ability to ship various products is in constant increase and presents itself as a relentless sector. Collectively, it is very important to have reliable means, namely vehicles and transport machinery. For that matter, one of the most popular uses of heat exchangers is in mechanical engineering. A very common use is for regulating temperatures around vehicle engines to prevent them from over-heating.

In the case of cars, this heat exchanger comes in the form of a radiator which contains a solution of water and ethylene glycol. The latter in fact possesses cooling properties since it is characterized by a very low freezing temperature. The radiator, with the aid of this ethylene glycol property, takes hot air generated by the engine and releases it with a cooler temperature in the ambient space surrounding the engine. The same concept can be projected, but on a bigger scale, onto airplane engines. The figure below shows a basic turbojet engine design: [4] [5]

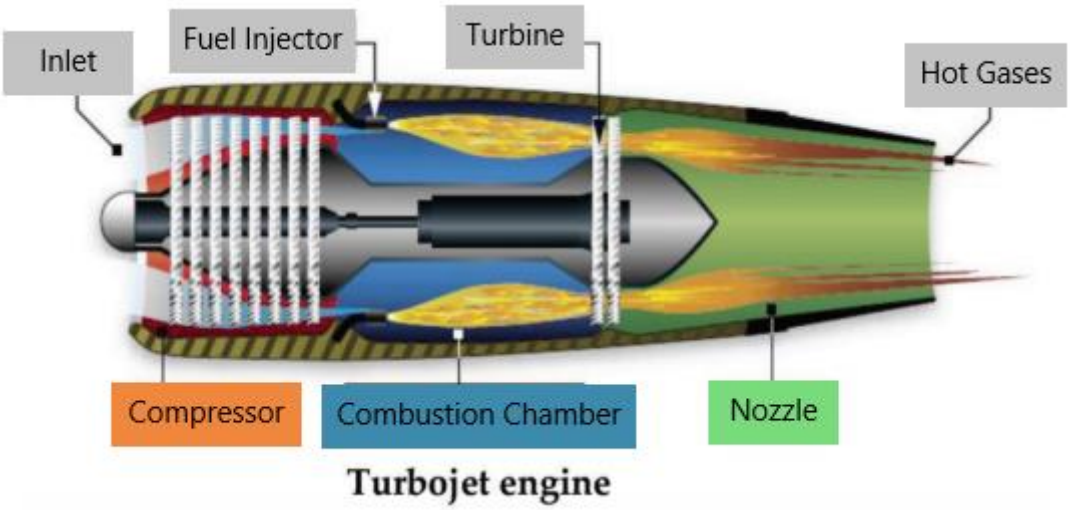

Figure 10: Basic design of a turbo-jet engine [5]

For this case, airplane engine cooling is done by the flow of cool air through the motor compartment. This air enters, at the inlet, from the openings of the engine cowling (which refers to its removable exterior covering) and is later expulsed as hot air from the lower section of the engine case. This process, once again, assures a safe functioning and operation of the entire plane by avoiding the overheating of the engine, and maintaining it at cool temperatures.

Although this process of turbojet engine cooling is less efficient during ground operations as well as take-offs and landings (due to of a combination of a low air velocity and a large power consumption during these operations), it still manages to provide efficient cooling for the engine during stable flying conditions, which usually last for longer durations than landing and take-off situations. As a matter of fact, while ground operations need a few minutes, flying time may take up to 24 hours, which calls for an extremely efficient and steady engine cooling system. [5]

3.2.3 In the food industry

Heat exchange is a very important part of the food industry. It provides manufacturers with a fast and simple way to preserve different kinds of foods by increasing their shelf life.

In this domain, the most favored type of heat exchanger is the plate heat exchanger. That is mainly because it is very simple to clean, sanitize and maintain at proper hygiene standards. As a matter of fact, thanks to its simple design, it is easily dismounted and cleaned. Moreover, its plates are usually made of stainless steel, making it compatible with the food industry requirements. [11] [15]

Before being packaged and loaded, the products are treated following the pasteurization method. It is a technique of preserving aliments by treating them with heat. In fact, the principle of the pasteurization technique states that microorganisms found in organic foods, and that are responsible for their natural fermentation and degradation can be eliminated by simply heating the product to a temperature slightly lower than its boiling point. The challenge is to maintain the product at this temperature for a certain time duration which can vary from one product to another. This is shown in Table 1. [9] [11]

As an example, treating milk requires holding it at a temperature of about 70°C for a minimum of 16 seconds. A few conditions of food treatment are summarized in the table below. [10]

Table 1: Pasteurization conditions [10]

Batch wise pasteurization	62-65°C for 30 minutes
High Temperature Short Time pasteurization (HTST)	72-75°C for 15-240 seconds
High Heat Short Time pasteurization (HHST)	85-90°C for 1-25 seconds

For the case of milk, a process called continuous pasteurization is used, and it usually involves heat exchangers that are composed of 3 main compartments: heating, holding, and cooling. A typical arrangement of these heat exchangers is illustrated in Figure 11. [3]

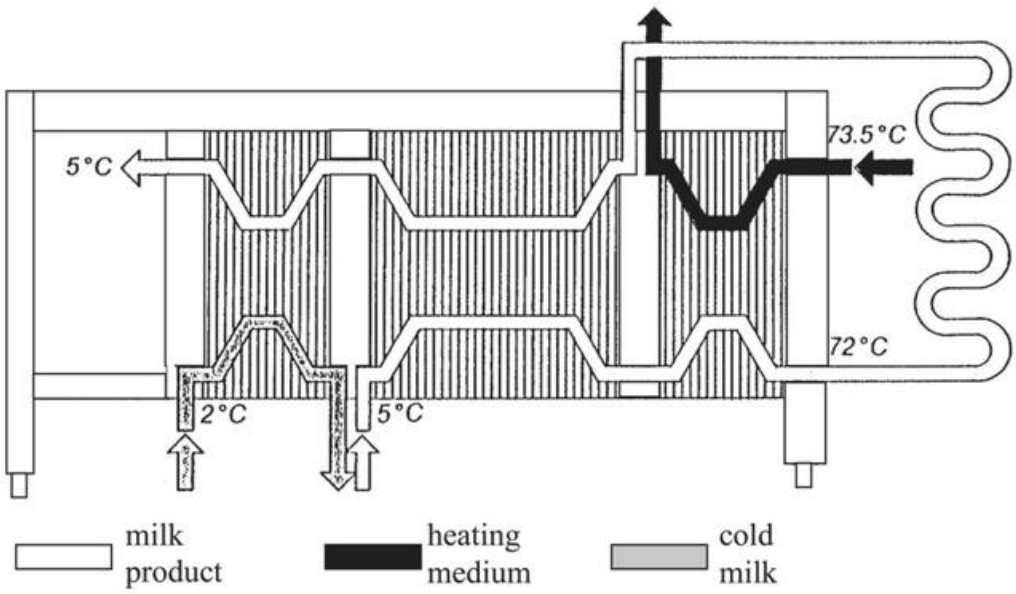

Figure 11: Configuration of a pasteurization HX [3]

First, the milk enters the heat exchanger as a raw product and under a cold temperature. In the heating compartment, it is heated until a temperature ranging from 57 to 68°C. This is done via an already pasteurized milk crossing the same section of the heat exchanger. After that, when the warm milk reaches the heating section of the heat exchanger (on the far-right side), it is further heated up to 72°C by the means of a heating medium like hot water or steam. See Figure 11. [3]

At this point, the milk is technically pasteurized. It travels again the middle section of the heat exchanger, but this time playing the role of the warm fluid and is consequently cooled down by the cold raw milk coming in, as mentioned at the beginning of the cycle. However, the temperature of the milk is not quite adequate for packaging. Thus, it is further cooled by the means of a cooling medium in the cooling section of the heat exchanger, until reaching a temperature of 5°C. [3]

3.2.4 In environmental engineering

The focus of environmental engineering is to pursue the reduction of human impact on the planet, the ecosystem, and the climate as much as possible when indulging in industrial practices.

Our environmental footprint, in general, has been put forth since a couple of decades when climate change, paired with the extinction of many fauna and flora species became clear. It is believed that the prime cause of this is uncontrolled greenhouse gas emissions. Thus, efforts have combined to monitor industrial activities in terms of their chemical releases, and to raise a sense of awareness about the effect of irresponsible toxic emissions on the longevity of the planet.

Thereupon, one of the principal duties of environmental engineering is to create new methods to control and reduce pollution, be it related to the contamination of water, air, soil or even underground resources. For that matter, heat exchangers happen to be eminent in the industry, as they have proven to solve many environmental-related problems such as

volatile organic component (VOC) release, wastewater discharge and solid hazardous industrial waste combustion. [16] [17]

Another way heat exchangers have been found to be efficient when treating this issue, is through exploiting eco-friendly and renewable means of energy production. This in fact is the optimum solution since waste and pollutant emissions are none. The most prominent example of this application are solar panels. These constructions are an alternative way for domestic heating using natural solar energy. Not only is this a great approach for minimizing the environmental impact, but it is also very cost-effective due its renewable nature, and to the fact that it relies mainly on a natural and endless source of energy. [18]

Solar panels are widespread and can be used either for potable water heating or for space heating. Although they procure heat by relying on solar energy, a lack of the latter lightly affects their performance, thanks to the heat storage quality of their collectors. This means that they are still useable during the winter season, on cloudy days and in colder parts of the planet. [19]

In substance, solar panels rely on heat exchangers to transmit solar heat that is stored in the collectors to water streams or ambient air within a household. Consequently, the design of the heat exchanger in this case can vary due to the diversity of its applications. The most adopted designs are coil-in-tank, shell-and-tube and tube-and-tube heat exchangers, with the latter being the most efficient. [19]

Below is a simplified illustration of the domestic water heating system using solar panels.

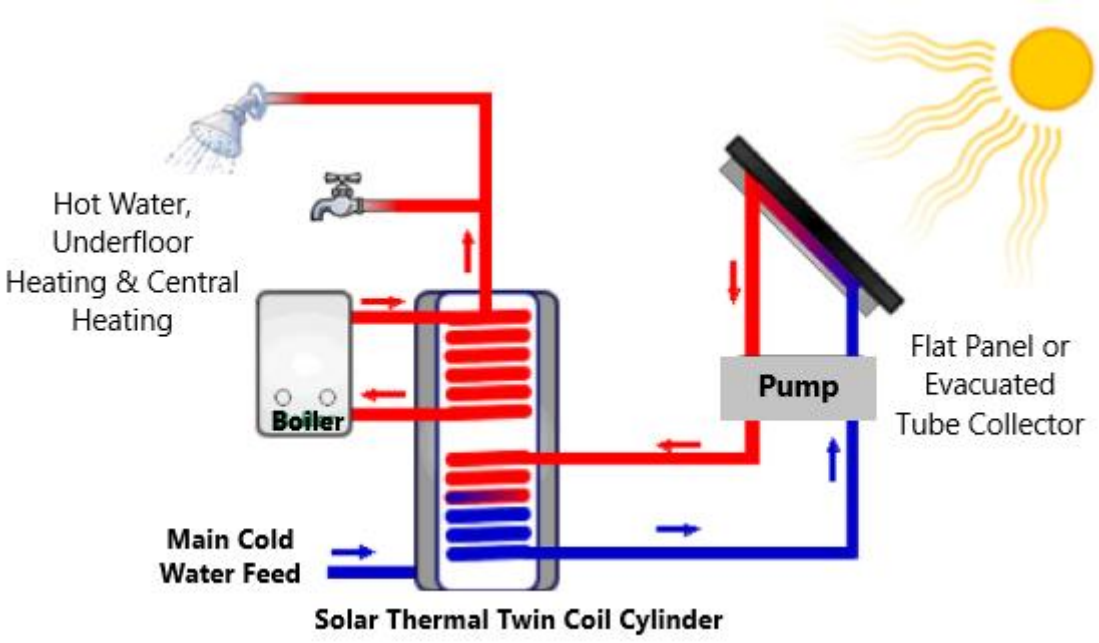

Figure 12: Solar thermal domestic water heating system [18]

As shown in figure 12, heating through solar energy is realized via a simple heat transfer between cold water entering from the feed and solar radiation.

These radiations are stored in the collectors in the form of heat. This is secured by the insulated and weather-proof nature of the collectors. Meanwhile, the cold water coming from

the feed is collected in the storage tank and will serve later as a heat-transfer fluid. It travels to the collectors and absorbs the heat stored there. The water is now hot tailing its contact with the collectors, so it flows back to the storage tank and there, it transfers heat to the locally stored cold water.

In this case, the fluid interaction is ensured by a coil-in-tank heat exchange system consisting of one or many coil tubings submerged in the storage tank.
Finally, the heated water leaves the storage tank. It is then pushed to the boiler and is ready for use. [19]

3.2.5 In the medical industry

Many medical tools and equipment are in need to be cooled in between uses. This need for implementing heat exchangers is in fact crucial in modern medicine whether it is to keep external temperatures of equipment safe for direct contact with patients, to maintain electronical medical devices in good shape or to cool down surgery instruments using the cryogenic method.

Using integrated heat exchangers in medical devices has proven to increase their efficiency and precision as well as their longevity. This is especially the case since the largest portion of medical equipment is sealed for sanitary reasons, making it difficult to use conventional external cooling methods. [16]

Most heat exchangers used in such practices are highly compact and finned on both sides in order to ensure maximum heat transfer for a limited surface area. However, the biggest parameter to look after in this case is the type of material used for construction, since the usually used materials for heat exchanger pipes can be dangerous for the human body. Typically, heat exchanger pipes are made from copper, but are swapped by plating from gold or nickel for cases of medical use. [16]

3.2.6 In the pharmaceutical industry

The pharmaceutical industry is a very sensitive field of practice that requires a great deal of precision. The quality and effectiveness of the end-product as well as its validation from consumers are paramount. They are usually assured by several standards such as quality control, process supervision, reliability of machinery and regular cleaning accompanied by maintenance as of a certain number of production cycles. [20]

During its life cycle, every chemical endures the following steps in order to be manufactured as a ready-to-use product, namely tablets:
- Dispensing
- Sizing
- Powder blending
- Granulation
- Drying and dry screening
- Tablet compression
- Coating

The required ingredients for tablet production are weighed and dispensed separately before moving on to sizing, where they are divided evenly. This aims to reduce their size in order to ensure an easy mixing procedure later. [22]

Subsequently, the blending process is carried out. During the latter, ingredients are finely blended to create a homogeneous powder. Next, during granulation, small layers of powder are combined via freezing. Then, the drying process takes place. This is where heat transfer comes to play. During this step, wet granules produced during granulation are to be dried for a certain period under controlled temperatures. This requires a process of sublimation, done under low pressure conditions to ensure that the solid granules reach the gas state directly without going through the liquid state. This is a process that is procured either via conduction through tray dryers and bed dryers, or via convection through heat exchangers. The challenge of the drying step lies in optimizing pressure and temperature conditions. The goal is to be able to reach a thorough sublimation at the boundary between the ice core and the chemical. In fact, as mentioned previously, low pressure conditions need to be established as a prerequisite for sublimation, because the latter occurs when a chemical component is situated at a pressure lower than its triple point pressure.
Meanwhile, convection is not possible at pressures under 10^{-2} mbar. For that matter, pressures during drying are adjusted to the highest value possible. This pressure is a function of the required temperature for sublimation. [21]

During this heat transfer process, external fluids are used for heating the chemical under the required temperature. But since it has already been established that when dealing with pharmaceuticals, quality control is of immense value, most manufacturers opt for safety barriers to prevent chances of cross contamination. [22]

Cross contamination is a common incident where the product is unintentionally mixed with the heat-transfer fluid either because of a leak or a failure occurring in the piping system. So, one way to mitigate this problem is by maintaining a positive pressure gradient which will make sure that the flow direction is from the product to the heat-transfer fluid, in the event of a leak. Alternatively, the better solution is the placement of a physical barrier separating the flow paths of both fluids, making it very difficult for them to mix even in case of a leak. [22]

Finally, the last two steps of the tablet manufacturing process consist of compressing the granules into the unique shape of the pill be it round, oblong, etc. And then to conceal unpleasant chemical tastes or odors if necessary. [22]

4 Heat Exchanger Design

4.1 Introduction to the ESP test stand

The chair of petroleum engineering at Montanüniversität Leoben owns a lab which is home to a pump testing facility. It is equipped with a collection of pumps used to perform artificial lift experiments.

Among the number of available pumps being tested is an electrical submersible pump (or ESP). During the tests performed with this pump, fluid entering the pump vessel at a pressure of 20 bar is compressed to 70 bar. This rise in pressure engenders a rise in temperature as well, this means that the fluid is now too hot to be handled by the pipe and especially to get in contact with the motor. This will ultimately lead to overheating within the motor, affecting the overall efficiency of the pump. That is where this study comes into practice.

As a matter of fact, the objective is to cool this fluid down and keep it at a constant temperature to prevent heating up the motor when they both eventually get in contact. ESP motors are indeed critical components of the electrical submersible system and are prone to many failures due to their sensitivity to overheating or power incompatibility. So, in essence, it is a system optimization problem by managing the demands of the machine in a way that they do not exceed the power generated by the system. Thus, avoiding crashes or failures.

The second station of the fluid would then be a disposal tank. It is meant to collect the fluid running through the pump, which is in this case the hot fluid, if it is not re-circulated into the system.

Therefore, there is a two-fold need for a heat exchanger: First, it increases the efficiency of the pump by maintaining the cooled fluid at a constant temperature. This means to protect the ESP motor by ensuring that the circulated fluid reaches it at reasonable heat. And second, it keeps the disposal tank from heating up.

4.2 Data and Primary Estimations

To be able to design a heat exchanger, the starting point is procuring basic information. For this type of problem, the principal parameters are the temperatures of the fluids. This allows an understanding of the degree to which a certain fluid needs to be cooled or heated. Then, parameters related directly to the device to be designed can affect for instance the rate of heat transfer, size and even power consumption.

Thus, as a start, we begin by identifying the inlet and outlet temperatures of both the hot and the cold fluid. This determines in a way the kind of heat exchanger we want to design in terms of heat transfer efficiency, its flow arrangement, power consumption required to meet the desired end results, etc.

As a first step, both fluids in the process need to be identified. The first fluid is being run through the ESP pump during testing. The pumping system applies pressure on the fluid causing to it rise. This rise in pressure is translated by an increase in the fluid’s temperature. Thus, we can refer to this fluid as the hot fluid, and it is to be cooled down. The hot fluid is in fact slightly salty water or brine, but in this study, we will assume it is normal fresh water for

simplification purposes. The possibility of using additives as a corrosion remedy may also be an option in the future.

There are no strict limits surrounding the exact temperatures of the hot fluid; its inlet temperature is between 15 and 60°C, while its outlet temperature should not exceed the limit of 50°C. Meanwhile, the fluid used for cooling is fresh water. It is then referred to as the cold fluid.
This leads us to the cold fluid. It is in fact fresh water originating from the tap, which usually comes in a stable predetermined temperature. In the region of Leoben, this temperature is set at 8.5°C, but we will consider it 10°C for simplification purposes. Although the exact intake temperature for this fluid is known, its outlet temperature is not restricted because our focus will be mainly on cooling the hot fluid.

The second step then is to identify the flow rates. Flow rates are crucial for design calculations to come. For the hot fluid, an operating range of 5 to 20 m^3/h is allowed, as for the cold fluid, its flow rate is not meant to exceed 2 m^3/h.

Table 2 below shows a summary of some of the available parameters from preliminary data regarding both fluids. Specific heat values are included to be used in further steps, and just as a primary indication of the heat transfer capacity of each fluid. Note that for the specific heat value of the hot fluid at Intake, an average temperature of 35°C was considered, versus 50°C at the outlet.

Table 2: Physical properties of used fluids

	Hot Fluid	**Cold Fluid**
Type	Salt water / water	Fresh water
Inlet Temperature [°C]	15 - 60	10
Outlet Temperature [°C]	Less than 50	-
Flow Rates [m^3/h]	5 - 20	Less than 2
Specific Heat @inlet (35°C) [J/kg.K]	4178	4194
Specific Heat @outlet (50°C) [J/kg.K]	4181	-

From a construction point of view with regards to the heat exchanger, a few design parameters are worth considering. For starters, we are constricted with size. Considering the lab offers limited space, size management is required. Thus, the projected dimensions of the device are a length of 5.5m and a width of 1m. These numbers are in fact maximum values which should not be exceeded due to space limitations. Nevertheless, smaller dimensions are possible if they fulfil the outcome results.

As for the type of the device, a pipe-in-pipe installation is suggested, while maintaining the structure as flat as possible. This directly implies minimal height and possibly no finning around the tubes. This would then be classified as a relatively compact heat exchanger, having an area density around or smaller than 700 m^2/m^3. Note that the area density usually

referred to as β is a parameter to measure a heat exchanger's compactness, and physically represents the ratio of the area of heat exchange over its volume. [1]
And finally, with regards to material, the discussion stands between steel and stainless steel as two viable and reliable options. On one hand, steel is more commonly used and much more affordable; this is especially helpful for a small-scale academic project. Moreover, it has excellent thermal conductivity resulting in better heat distribution. In addition, it is lighter than stainless steel, which simplifies handling and transport. On the other hand, stainless steel offers a high protection against any risk of corrosion. After all, we are dealing with partially salted water, meaning that chances of damage to the material are never zero. This may include corrosion, erosion corrosion, galvanic corrosion and even bacteria growth.

In addition, this choice of material comes with minimal maintenance and lower frequency of interventions resulting from the problems mentioned above. Yet after discussion, the choice was set on regular steel due to its practicality and affordability.

The following point ticks the box of power requirements. It is indispensable for any heat exchanger design process to make sure power consumption is within norms. This is important because the costs of energy consumption, in many cases, can add up on the long run making it more expensive than manufacturing itself. Consequently, it is wiser to spend more on manufacturing the heat exchanger while saving energy later.

This brings us to the last point which is the total cost of manufacturing. We are within the restrictions of a budget of 4000€. In order to remain within these bounds, power consumption, material of design and size will all need to be monitored during the design process.

As a primary estimation, the main challenges along the course of the design phase can be classified into two groups: physical challenges and practical challenges. Parameters that fall into the group of physical challenges may include the size of the heat exchanger itself. Is the calculated length of the heat exchanger, which is supposed to ensure an efficient heat transfer, in harmony with the dimensions of the lab? And by the same token, if we restrict ourselves with a certain length for the heat exchanger, proportionate with the lab dimensions, are we going to get optimum desired heat transfer rates?

Size also encloses pipe diameters inside which both fluids will flow. Not only do these pipe dimensions have to be in congruence with the size of the heat exchanger per se, but also chosen diameters must be able to support fluid flow rates, have an appropriate thickness that allows an efficient heat transfer between the fluids with minimal wall resistance, and finally ensuring convenient pressure conditions for the transport of fluid and safety of the pipes at the same time. This of course includes considerations for thermal and structural stresses accompanied with certain heat and pressure conditions.

Further with regards to practical challenges, even the best engineered designs may not apply as accurately in the field. One factor could be the influence of the surrounding room temperature. It can vary according to seasons, or even the activity taking place within the vicinity; presence of other equipment, heat released from radiators, etc.

For that matter, it is vital for the continuity of the project that priorities be well defined and set in accordance with the role that the heat exchanger is meant to accomplish.

4.3 Design Calculations

4.3.1 Method choice: e-NTU method

As mentioned before, there's a couple of different approaches to take when designing a heat exchanger. The primary factor that favours one method over the other is the initial data that we have available coupled with our desired end goal.

First in the list is the LMTD method, which is short for the Logarithmic Mean Temperature Difference method. It is based on the principle that the difference in temperatures between the hot and the cold fluids varies along the length of the heat exchanger, hence defining a mean temperature difference noted ΔT_{lm} , and which can be defined by the following relation:

$$\Delta T_{lm} = \frac{\Delta T_1 - \Delta T_2}{\ln\left(\Delta T_1 / \Delta T_2\right)} \qquad \text{(Eq. 1)}$$

This method is ideal in the event where both inlet and outlet temperatures are known or can be deduced using an energy balance. Correspondingly, the goal in the end of this workflow is to determine the size of the heat exchanger. [1]

At first glance, the LMTD method seems like the ideal way to solve our problem, yet it does not really get us anywhere since our initial data comprises of two unknown temperatures, out of a total of four. The referred to temperatures are both outlet temperatures of the two fluids. Although that of the hot fluid is given in the form of an interval, it is not enough for us to calculate the log mean temperature difference, which is evidently the basis of the LMTD method.

On a second level, the next step would be to determine the surface area with given heat transfer rate $\dot{Q}$ and overall heat transfer coefficient U which is to be calculated in our case.

Secondly, we have the Effectiveness-NTU method, or e-NTU method. Essentially, it was developed to determine either the heat transfer performance or its efficiency for an already existing heat exchanger. Equivalently, it is referred to in many cases to decide whether an available heat exchanger can accomplish a desired job. Thus, it is optimal in cases where the heat transfer rate and outlet temperatures are to be determined, while inlet temperatures and mass flow rates of both fluids are given. [1]

It is also suitable when both the type and the size of a certain heat exchanger are known. In our case, although we have settled on a pipe-in-pipe heat exchanger with a counter-flow arrangement, the size remains a variable but within the range of 10 by one meter. [1]

Due to the reasons mentioned above, the e-NTU method was found more fitting for use. It is fair to note that the LMTD method is of valid use in this study particularly, yet it requires very complicated iterations which can overwrite its ability to solve the problem.

In fact, calculations at the beginning of approaching this heat exchanger design task were quite crippling due to the huge number of variables that resulted in turn in infinite pools of possibilities. For that matter, the e-NTU method was developed and is used to simplify calculations.

An example of these iterations would be to try multiple combinations of temperature differences, by assuming different values of outlet temperatures each time. As a result, one will end up with a large range of values for ΔT_{lm} that needs to be verified with calculations. Many of them can be excluded, if not deemed absurd, purely due to physical reasons that lie within the configuration itself.

For instance, for a counter-flow configuration, the outlet temperature of the cold fluid can exceed the outlet temperature of the hot fluid, but never under any circumstances does it exceed the inlet temperature of the hot fluid. [1]

The same reasoning is applied for all invalid cases, as well as the overall heat transfer coefficient calculations in a further step.

4.3.2 Workflow:

As discussed in the previous section of this chapter, opting for the e-NTU method appears to be a better option, since the LMTD method workflow requires loads of iterations, making it very difficult to use and not quite fit for our task. Also, considering the primary data that we have at hand, the effectiveness-NTU method appears to be more adequate, as it is acknowledged in literature for being the better choice in the event where the type, size or surface area of the heat exchanger are known while its outlet temperatures are to be calculated.

Heat exchangers calculations require the use of the overall heat transfer coefficient U, which a very important parameter. It can be best described as the ability of a barrier to transfer heat. The barrier being usually a combination of convective and conductive environments or surfaces. [12]

The following contains a walk-through and a detailed explanation of the steps of calculations that what were used in the problem-solving workflow. The first work package aims to calculate the effectiveness ε of the heat exchanger and its Number of Transfer Units (NTU). This is a parameter which the e-NTU method is based on, hence the name.
But first, it is necessary to determine a few physical and thermal properties of the fluids.

Step 1: Calculating the heat capacity.

Flow rates of both the hot and the cold fluid are available to us. So, starting from this point, we can calculate the mass flow rate $\dot{m}$ [kg/s] for each fluid using the following relation:

$$\dot{m}=q\rho_w \quad \text{(Eq. 2)}$$

with q [m^3/h] being the flow rate of the fluid, and ρ_w [kg/m^3] the density of water at a standard temperature, estimated by 4°C. This value is rounded to 1000 kg/m^3 for simplification purposes.

This enables to calculate the heat capacity rate C [w/k], which is defined as the rate of heat transfer needed to change the temperature of the fluid stream by 1°C while flowing through a heat exchanger. [1]

The heat capacity rate can be calculated as follows:

$$C = \dot{m}c_p \quad \text{(Eq. 3)}$$

Where c_p [J/kgK] is the specific heat of the fluid. It is specific for each fluid and highly depends on the temperature. In this study, considering that large intervals of inlet temperatures are experienced, it is much more convenient to use an average value of heat capacity instead of a unique value for each temperature individually. Given values of temperature are ranging from 10 to 60°C, therefore, an average value of all heat capacity values associated with our temperature range was used. The average heat capacity value used is then 4184,0909 J/kgK.

From the heat capacity rate, C_{min} can be deduced, which is the minimum value of heat capacity rate among both fluids. Since the hot fluid has higher initial flow rates, and therefore higher mass flow rates ṁ, the minimum value of heat capacity among both fluids is always associated with the cold fluid. In other words, C_{min} is always that of the cold fluid.

The previous workflow was indeed used as a guideline to perform the calculations in Excel. This is notably shown in figure 13 below. The workflow kicks off on the left side by choosing input data, which are marked by green cells. It then moves its way across to the right side, as the physical and thermal properties of both fluids are calculated. The first step of calculations illustrated in figure 13 is concluded by determining the capacity ratio c, which is a dimensionless parameter that is useful for upcoming calculations.

Q̇ [kw]	qc [m³/h]	qh [m³/h]	ṁ_c[kg/s]	ṁ_h [kg/s]	Ch[w/k]	Cc[w/k]	Cmin[w/k]	Cmax[w/k]	c
9	0.3	2	0.08333333	0.5555556	2324.49495	348.674242	348.67424	2324.4949	0.15

Figure 13: First step of fluid properties calculations

Step 2: Calculating effectiveness and NTU.

Using the first law of thermodynamics, it is possible to calculate the maximum heat transfer rate, $\dot{Q}_{max}$ from the heat capacity.

$$\dot{Q}_{max} = C_{min}\Delta T_{max} = C_{min}\left(T_{h,in} - T_{c,in}\right) \quad \text{(Eq. 4)}$$

In the former relation (Eq. 4), there has been in fact recourse to the minimum value of heat capacity rate among both fluids because the fluid with the smaller heat capacity rate is the one to witness the larger temperature change first, consequently, it is the first to reach the maximum temperature. [1]

For the design of this heat exchanger, a counter-flow heat exchanger was chosen. Although the cooling rate of the hot fluid for the case of a counter-flow heat exchanger is slower than that of the parallel-flow case, they are usually preferred in practice due to their flexibility in size and dimensions. In fact, for counter-flow heat exchangers, both fluids enter the device from opposite sides. The immediate consequence of that is a higher value of log mean temperature difference ΔT_{lm} compared to parallel-flow heat exchangers, as detailed in equation 1. This implies that in order to reach a certain heat transfer rate, a smaller heat transfer area is required for a counter-flow heat exchanger in comparison to a parallel-flow heat exchanger. [1]

Figure 14 below illustrates temperature variations of both the hot and the cold fluid for the case of a counter-flow heat exchanger.

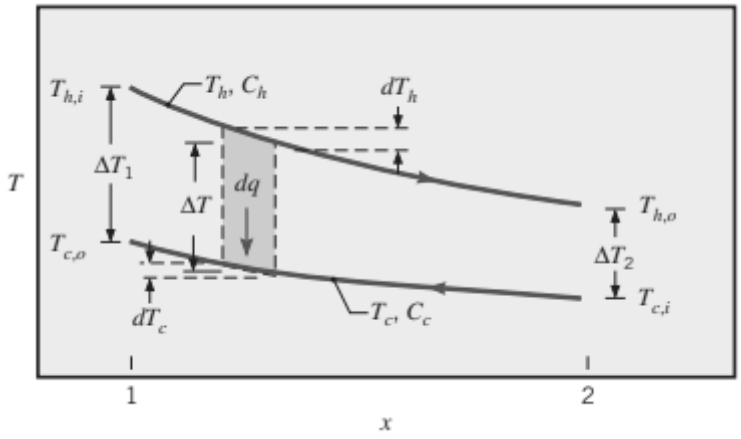

Figure 14: Temperature profile in a counter-flow HX [2]

The figure above seems to be in accordance with the relation expressed in (Eq. 4). In fact, maximum temperature difference ΔT_{max} is the difference between the temperature of the hot fluid and that of the cold fluid, both at the inlet. It is at this point in the system where both fluids have experienced the least (if at all) heat transfer possible, be it gained or lost. [1]

Coming to the effectiveness, it is a dimensionless parameter that depends on the geometry and the flow arrangement of the heat exchanger. It is in fact a very useful parameter when trying to determine heat transfer rates without having the outlet temperatures of a heat exchanger. [1] It is defined as follows:

$$\varepsilon = \frac{\dot{Q}}{\dot{Q}_{max}} \quad \text{(Eq. 5)}$$

With Q̇ [kW] here being the actual heat transfer rate and can be determined from an energy balance of either fluid, at any point in the system. In our case, the actual heat transfer rate is the power supplied by the pump, and that we have defined in the range of 5 to 55 kW.
As one would expect, values of effectiveness should range between 0 and 1.

Once this is done, we can move on to calculate the NTU value. This parameter, known as the Number of Transfer Units, is in fact the parameter which the effectiveness-NTU method was based upon and derives its name. It is crucial for determining the total area of heat transfer characterizing a heat exchanger, and therefore deducing its length. NTU is a dimensionless parameter and can be defined accordingly: [1]

$$NTU = \frac{UA_S}{C_{min}} \quad \text{(Eq. 6)}$$

Due to the fact that both the overall heat transfer coefficient U and the surface area of heat transfer A_S are unknown, it is not possible to use the definition of NTU for our calculations. Instead, we will refer to effectiveness relations that were developed practically by William M. Kays, 1984. In these relations, a few possible formulas are available for calculating the effectiveness when given NTU and the capacity ratio c. After defining the capacity ratio as follows:

$$c = \frac{C_{min}}{C_{max}} \quad \text{(Eq. 7)}$$

we can proceed to calculating NTU via effectiveness relations. It is possible to resort to the relation that ties effectiveness and the number of transfer units together, developed specifically for the case of counter flow heat exchangers:

$$\varepsilon = \frac{1 - e^{-NTU(1-c)}}{1 - c\, e^{-NTU(1-c)}} \; for\; c > 1 \quad \text{(Eq. 8.a)}$$

$$\varepsilon = \frac{NTU}{1 + NTU} \; for\; c = 1 \quad \text{(Eq. 8.b)}$$

Therefore, manipulating the previous relations to extract NTU leaves us with the following expressions:

$$NTU = \frac{-\ln\left(\frac{1-\varepsilon}{-c\varepsilon + 1}\right)}{1 - c} \; for\; c > 1 \quad \text{(Eq. 9.a)}$$

$$NTU = \frac{-\varepsilon}{\varepsilon - 1} \; for\; c = 1 \quad \text{(Eq. 9.b)}$$

It is important here to note that NTU and ε are logarithmically related to one another, meaning that the more NTU increases, the less ε increases. Physically, this is synonym to a slow increase of effectiveness corresponding to large increases in NTU, but only beyond a critical value, which is usually around 3 by a rule of thumb. In other words, higher heat transfer rates are not always aligned with good economical choices, and since effectiveness reflects the geometry of the heat exchanger, it is safe to say that large heat exchangers are not necessarily a wise economical choice, as they are not always synonym to higher heat transfer rates. [1]

This series of calculations was also carried out in Excel. This is particularly presented in figure 15 below, where inlet temperatures of both fluids are input, while their outlet temperatures are calculated using (Eq.4). The input of data in Excel throughout the entire calculation procedure was done via controls, usually found under the "Developer tab". The use of controls is very flexible and practical as it regulates the range under which input values vary. Moreover, it allows a control over the increment separating two consecutive values. But most importantly, from a user's point of view, it provides a better interface, and a much easier way to handle data.

The second step of the calculations is then finished off by determining the effectiveness ε as well as the NTU.

Tc, in [°C]	Tc, out [°C]	Th, in [°C]	Th, out [°C]	ΔT_{max} [°C]	Q_{max} [kW]	ε	NTU
13.14	38.9520587	39	35.1281912	25.86	9.01671591	0.99814612	7.2097444

Figure 15: Second step of fluid properties calculations

Step 3: Calculating convective heat transfer coefficients h.

Alongside, calculating the convection heat transfer coefficient h is needed. Convective heat transfer is one of the most common forms of heat transfer. It occurs usually within fluids in general due to a molecule movement in bulks. Estimating the heat transfer coefficient is tricky mainly as it is highly sensitive to temperature. [2]

Since we are working in non-thin wall conditions, we need to assign two distinct values of the convection heat transfer coefficient: one for the hot fluid flowing inside the inner pipe, and the second for the cold fluid flowing in the outer pipe. They are noted h_i and h_o respectively.
The procedure for these calculations is in fact identical, the only variation lies in the diameters to be considered. But primordially, we must make a few preliminary calculations to be able to conclude the convection heat transfer coefficient. These calculations are primarily descriptive of fluid properties.

First, we are to evaluate the average velocity in the pipes using the following relation:

$$V = \frac{\dot{m}}{\rho_w \, \pi \frac{d^2}{4}} \qquad \text{(Eq.10)}$$

With $\dot{m}$ [kg/s] here being the mass flow rate of one of the defined fluids, in our case the hot or the cold fluid. ρ_w [kg/m^3] being the water density at standard conditions, and d^2 [m] being the inner diameter of the inner pipe squared for the case of the hot fluid, and the difference between the inner diameter of the outer pipe squared and the outer diameter of the inner pipe squared for the case of the cold fluid. This in fact translates the flow of the cold fluid within the annulus of both pipes according to our model.

Then, we proceed to calculate Reynolds number, which serves to define the type of flow we have. We assumed that values of Re below 2300 indicate a laminar flow, whereas cases of turbulent flow are associated with Re values above 4000. [1]
Reynolds number is defined as follows:

$$Re = \frac{Vd}{v} \quad \text{(Eq.11)}$$

Here, V [m/s] is the previously calculated average velocity, d [m] is the inner diameter of the inner pipe for the case of the hot fluid, and the difference between the inner diameter of the outer pipe and the outer diameter of the inner pipe for the case of the cold fluid. Finally, v [m²/s] being the kinematic viscosity, which depends solely on the fluid temperature.

According to the results of the calculations, the fluid flow within the pipes of the heat exchanger is characterized by a turbulent flow most of the time, therefore in the upcoming steps, the workflow for cases of laminar flow will be disregarded.

The following step requires calculating the Nusselt number for cases of turbulent flow using the following relation:

$$Nu = 0.23\ (0.8\ Re)\ Pr^{0.4} \quad \text{(Eq.12)}$$

In (Eq. 12), the Nusselt number is calculated based on the Prandtl number and the Reynolds number as variables. With Pr being the Prandtl number, which is a temperature-dependent parameter. The previous equation contains only dimensionless parameters, namely Nusselt number, Reynolds number and Prandtl number. This is in fact a characteristic of a forced convection phenomena taking place in this process rather than a natural convection which would otherwise evaluate the Nusselt number depending on both Reynolds number and Grashof number. [23]

Note that for cases of laminar flow, Nusselt number is directly taken from a given list of values without preliminary calculations, as opposed to our case of turbulent flow where it must be evaluated as shown in (Eq. 12).

Once this is complete, we can proceed to calculate the convection heat transfer coefficients by the means of this relation:

$$h = \frac{kNu}{d} \quad \text{(Eq.13)}$$

K [W/mK] here is the thermal conductivity. It depends on the fluid temperature. Since the values of thermal conductivity corresponding to the given temperature intervals are extremely close, a single value of K was assumed throughout all the calculations for the sake of simplification. It is in fact an average value of all the possible thermal conductivity values that lie within our temperature range.

The same goes for evaluating both the average velocity of the fluid and the Prandtl number present in equations 11 and 12, respectively. Both parameters are highly dependent on the temperature of the fluid. Figure 16 below shows the procedure used for setting the values of these parameters.

Tavrg, h [°C]	Tavrg, c [°C]	Pr, h	Pr, c
37.064096	26.046029	4.83	6.14
		k [W/m.K] h	k [W/m.K] c
		0.623	0.607
		v [m²/s] h	v [m²/s] c
		7.20E-07	8.91E-07

Figure 16: Setting the thermal properties of the fluids.

Figure 16 highlights that the Prandtl number, the conductivity of the fluid as well as the kinematic viscosity are chosen based on the average temperature of the fluid. This average temperature is calculated from the inlet and outlet temperatures of each fluid, and the previously stated parameters are then picked in accordance with it. That is accomplished via an “IF” function, where each temperature interval is assigned a specific value of the mentioned parameters.

Nu is the previously calculated Nusselt number, for each fluid separately. Lastly, d [m] is the inner diameter of the inner pipe for the case of the hot fluid, and the difference between the inner diameter of the outer pipe and the outer diameter of the inner pipe for the case of the cold fluid.

The workflow described above is also shown in the following figure 17. Here, both the Reynolds number and the velocity are used to derive the heat transfer coefficient, the Nusselt number and the flow pattern relative to each fluid.

V [m/s] hot	V [m/s] cold	Re (hot)	Re (cold)	In case of turbulent flow:	Nu,h	Nu,c	hi [W/m².K]	ho [W/m².K]
1.0463836	0.414466	3.78E+04	1.86E+03		1.98E+02	1.96E+01	4.75E+03	2.98E+03
		turbulent	laminar					
				In case of laminar flow:	Nu,h	Nu,c	hi [W/m².K]	ho [W/m².K]
					5.0946667	4.9746667	122.07605	754.90567

Figure 17: Reynolds number, Nusselt number and heat transfer coefficient calculation

Following this milestone, the next package of calculations will include resistance calculations as well as wall area calculations. This aims to determine overall heat transfer coefficients, and ultimately the total surface area of heat transfer. Therefore, the use of the overall heat transfer coefficient relation is of best interest because it includes all the previously mentioned variables, necessary to our study.

Step 4: Calculating resistance R and overall heat transfer coefficients U.

Below, a basic network of heat transfer between two fluids in a double pipe heat exchanger is illustrated for a better understanding of the mechanism and the different parameters in play.

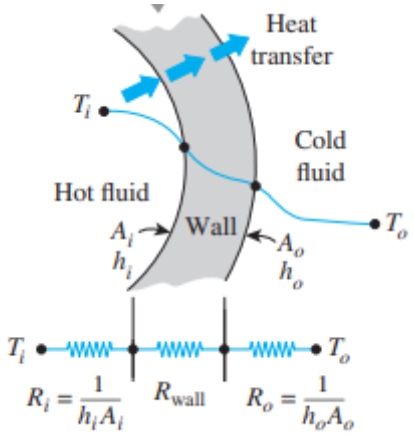

Figure 18: Heat transfer path and parameters in a double-pipe HX [1]

The heat transfer (or heat loss) in this system occurs from the hot fluid to the cold fluid. This process takes place thanks to convective heat transfer within the fluids, but also due to conduction occurring within the pipe walls. This is expressed in the thermal conductivity of steel. [1]

As previously mentioned, the optimal way to determine wall resistances and wall areas in the system is via the overall heat transfer relation. Figure 18 shows the significance of these parameters in determining the overall heat transfer coefficients of both fluids on a primary level, and the heat transfer area on a second level.

The overall heat transfer coefficient relation in equation 4 is valid for unfinned double-pipe heat exchangers, and can be expressed as follows:

$$\frac{1}{UA_s} = \frac{1}{U_i A_i} = \frac{1}{U_o A_o} = R_{total} = \frac{1}{h_i A_i} + \frac{1}{h_o A_o} + R_{wall} \qquad \text{(Eq. 14)}$$

Starting with area terms in this equation, A_s, A_i and A_o are respectively the total surface area of heat transfer, the inner area of the inner pipe wall and the outer area of the inner pipe wall.

Although evaluating A_s is the ultimate task of our calculations, both A_i and A_o can be calculated immediately at this point using the following relations, while assuming a unit length of 1m:

$$A_i = \pi \, l \, d_{i,i} \quad \text{(Eq. 15.a)}$$

$$A_o = \pi \, l \, d_{i,o} \quad \text{(Eq. 15.b)}$$

Moving on to the resistance terms, we can distinguish R_{total} and R_{wall} as total heat resistance within the system and heat resistance of the wall, respectively. In this case, the wall resistance is that of the inside pipe since heat is travelling from the hot fluid to the wall separating both fluids, and on to the cold fluid in that order.

The resistance of the wall R_{wall} can be then calculated via the following expression:

$$R_{wall} = \frac{\ln\left(\frac{d_o}{d_i}\right)}{2\pi k l} \quad \text{(Eq.16)}$$

Since this is meant to quantify the heat resistance of the wall, d_i and d_o refer to the inside and the outside diameters of the inner pipe. Meanwhile l is the length of the pipe, and k is the thermal conductivity of steel estimated by 22.5 W/m.K. [14]

On the other hand, the subtle resistance terms in equation 14 are: R_i which refers to the resistance of the fluid within the inner pipe, and R_o referring to the resistance of the fluid inside the outer pipe. Both these terms are expressed accordingly:

$$R_i = \frac{1}{h_i A_i} \quad \text{(Eq. 17.a)}$$

$$R_o = \frac{1}{h_o A_o} \quad \text{(Eq. 17.b)}$$

On this basis, equation 14 can therefore be boiled down to the following relation:

$$R_{total} = \frac{1}{h_i A_i} + \frac{1}{h_o A_o} + R_{wall} = R_i + R_o + R_{wall} \quad \text{(Eq. 18)}$$

Consequently, we can now calculate the total resistance in the system by simply summing up all the previously calculated resistance terms through equations: Eq. 16, Eq. 17.a, and Eq. 17.b. From there, we can deduce the overall heat transfer coefficients for both fluids through this expression:

$$\frac{1}{U_i A_i} = \frac{1}{U_o A_o} = R_{total} \quad \text{(Eq.19)}$$

Hence:

$$U_i = \frac{1}{R_{total}\, \mathrm{A}_i} \quad \text{(Eq. 20.a)}$$

$$U_o = \frac{1}{R_{total}\, \mathrm{A}_o} \quad \text{(Eq. 20.b)}$$

Once again, the same workflow was adopted in the Excel calculations, which can be seen in figure 19 below.

				Inner pipe		Outer pipe									
k (Stainless St	hi	ho	l unit	Di	Do	Di	Do	Ai	Ao	Ri	Ro	Rwall	R	Ui	Uo
[W/m.K]	[W/m²K]	[W/m²K]	[m]	[m]	[m]	[m]	[m]	[m²]	[m²]	[°C/W]	[°C/W]	[°C/W]	[°C/W]	[W/m²K]	[W/m²K]
22.5	4749.9255	754.905667	1	0.026	0.03	0.034	0.038	0.0816814	0.0942478	0.0025774	0.0140552	0.001012231	0.0176449	693.83906	601.327187

Figure 19: Resistivity and overall heat transfer coefficient calculations

In figure 19, pipe dimensions are input in the calculations. These dimensions refer to the inlet and outlet diameters of both pipes (inner and outer pipe), and are entered in the cells marked in green. The heat transfer coefficients calculated in the previous step serve as an aid to conclude the thermal resistance of the wall as well as the overall heat transfer coefficients on both ends of the wall.

Step 5: Calculating the length.

The final calculation package aims to estimate the size, or the length of the heat exchanger. Thus, we need to first calculate the total surface area of heat transfer, by recourse to NTU. For that matter, equation 6 can be rearranged to give the following relation:

$$A_s = \frac{NTU\ C_{min}}{U} \quad \text{(Eq. 21)}$$

Where NTU is the Number of Transfer Units, U is the overall heat transfer coefficient and $\mathrm{C_{min}}$ is the minimum heat capacity which has already been defined in step 1.

Note that in equation 21, we used the overall heat transfer coefficient for the hot fluid (U_i) because the heat transfer rate used throughout the calculation process is driven by the pump which pushes the hot fluid into the heat exchanger for it to begin the cooling process. In addition, the overall heat transfer coefficient of the system is not known, therefore that of the hot fluid is assumed.

Lastly, we can calculate the length of the heat exchanger from the total surface area of heat transfer through this expression:

$$L = \frac{A_s}{\pi d_{i,i}} \quad \text{(Eq.22)}$$

The term $d_{i,i}$ indicates the inside diameter of the inner pipe. The associated calculation procedure in Excel is exhibited in the following figure 20:

Ui.Ai	Uo.Ao	As [m²]	L [m]
56.6737522	56.67375224	3.623105552	44.3565506

Figure 20: HX surface area and length calculations

The first two cells are the product of the surface area and the overall heat transfer coefficient on each end. Both these parameters were calculated in the previous step and can be seen in figure 20, yet they only serve here as a verification.
Next, the surface area and the length of the heat exchanger can be determined with reference to equations 21 and 22, respectively.

Finding the length of the heat exchanger marks the finish line for the e-NTU method workflow. In fact, as mentioned in the beginning of this chapter, having recourse to the e-NTU method workflow aims to compute a heat exchanger's length based on initial data including inlet temperatures and flow rates of both the hot and the cold fluid as well as the heat transfer rate procured by the ESP pump. It is an ideal method to follow when figuring out the efficiency of heat transfer within a pre-existing heat exchanger, or for evaluating a heat exchanger size based on its fluid properties which makes it more eligible for our study. [1]

The following step would be to assess these results. One way to do that is to create a flow simulation inside the heat exchanger using OLGA software. The idea is to compare results of both methods to each other in order to evaluate their accuracy, and to weigh in on possibilities of improvements.

5 Simulation

5.1 Workflow

OLGA is a multiphase flow simulator which comes in handy for this study in order to showcase fluid behaviour, in addition to predict future fluid temperatures under certain conditions. This simulation is done using the 2018 version of the Schlumberger software OLGA.

The purpose of using OLGA in this study is to confirm the design of the heat exchanger, but from a different perspective. As a matter of fact, it aims to compare simulation results with design calculations that are based solely on theory, either to assess the accuracy of the theoretical model, or to validate the results and confirm its viability. In addition, it is perceived as a much more flexible tool since it makes changing design parameters very simple.

The procedure consists of recreating in OLGA the same conditions in which the designed heat exchanger operates. Conclusions can therefore be drawn in relation to the differences and to the similarities between both models, while showcasing the underlying reasons which might explain them.

Naturally, finding differences between both models is inevitable since both methods operate according to different workflows. In addition, OLGA has a numerous number of integrated models that can solve many hidden calculations for specific conditions, as opposed to Excel which is based on straight-forward thermodynamics.

An example of that would be accounting for the Joule -Thompson effect on the simulator's end, while for instance, the results of this effect can be portrayed as errors in Excel. This is because most fluids will experience a decline in temperature upon expansion like when travelling from a smaller to a larger volume of space. Although this phenomenon is recognized by the software, hand-calculations fall short to identify it and might even portray inexplicable changes in temperatures. [12]

5.2 Modelling

In this chapter, a walk-through of the OLGA model is laid out. It is used as a comparison for results stemming from the e-NTU method calculations. OLGA, being a multi-phase flow simulator is accompanied with various models integrated in the calculation process. These models may in this case offer more precise results than those obtained from pure theory.

First and foremost, defining initial conditions is cardinal. In this description, the order in which the folders of the model browser are displayed in OLGA was taken as a guideline.
Below is a representation of the main folders to be considered from the model. Each contains initial data with regards to the fluids, the pipes and even the configuration of the system. The ensemble of these folders constitutes then the input section of this simulation.

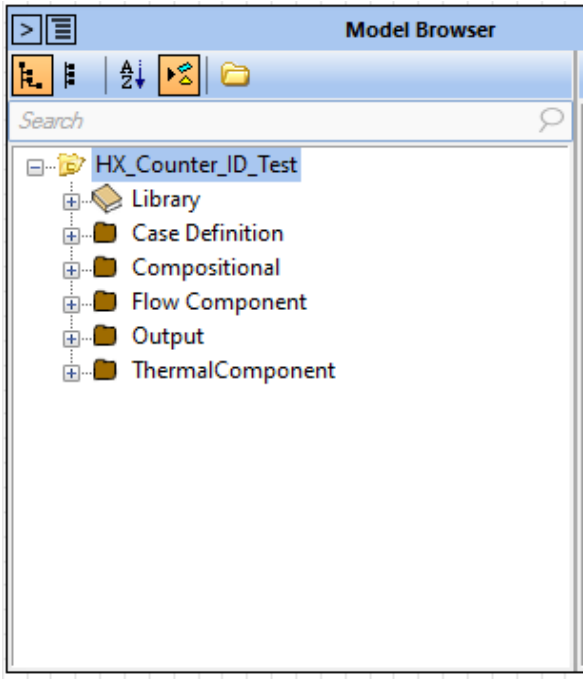

Figure 21: Model Browser Lay-out

First up is the “Library” folder. In this folder, the structural aspect is revealed. It describes material properties as well as pipe walls. The chosen pipe material is steel with a conductivity of 22.5 W/m.k, a capacity of 460 J/kg.k and a density of 7900 kg/m^3. The former values were taken arbitrarily from the steel properties table. [14]

Additionally, a second material was introduced to the model. This can be seen in the following figure 22:

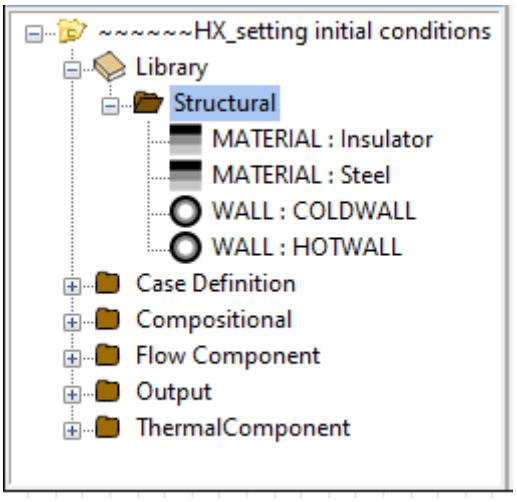

Figure 22: Layout of the "Structural" folder

Given the name “Insulator”, it is characterized by a very low conductivity and it has the purpose of creating insulation conditions like those of the hand-calculation step.

As a matter of fact, the thermal interaction between the outer environment and the cold fluid flowing in the outer pipes is not accounted for in the e-NTU method. Thus, the system comprised of the two fluids is thermally isolated from ambient air.

Then, a description of the walls is necessary. This refers to the wall dividing both fluids on one hand, and the wall dividing the cold fluid from ambient air on the other hand (see figure 22). Both walls are considered 2 mm thick and made of steel material.

The second folder to be discussed is the “Case Definition” folder. Its layout can be seen in figure 23 below.

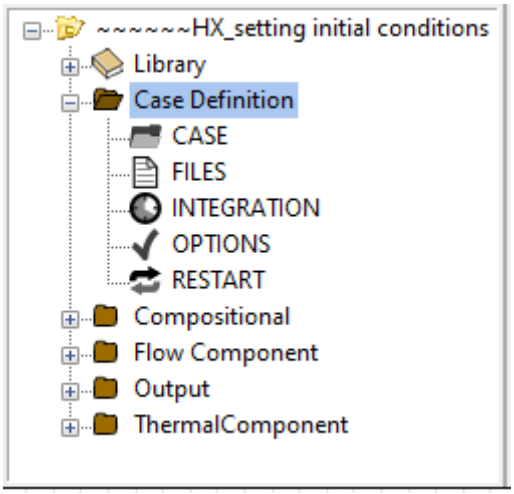

Figure 23: Layout of the "Case Definition" folder

Among the components of this folder, “Integration” and “Options” are worth pointing out. In fact, while the first focuses on the type and the runtime of the simulation itself, the latter sheds the light on the multi-phase aspect of fluids to be simulated, in addition to the models used by OLGA for simulating.

Starting with “Integrations”, a transient state flow was opted for as it allows creation of profiles at different points in time in order to illustrate the change that occurs in a certain parameter through the course of time. Here, the duration of the simulation was set at 60 seconds, with a maximum time-step of 0.5 seconds and a minimum time-step of 0.001 seconds.

Meanwhile in the “Options” section, it is important to note that a compositional tracking is allowed when the compositional option is activated. The black oil model is used in this instance and the number of phases to be simulated is fixed at three, which happens to be the only option in this version of OLGA.

Furthermore, an extension of this is represented in the subsequent folder named “Compositional”. Despite water being the only phase available in practical terms, three phases have been simulated. In the “Compositional” section, each phase is dealt with

individually under the “Black Oil Component” sub-folders. This is presented in figure 24 below.

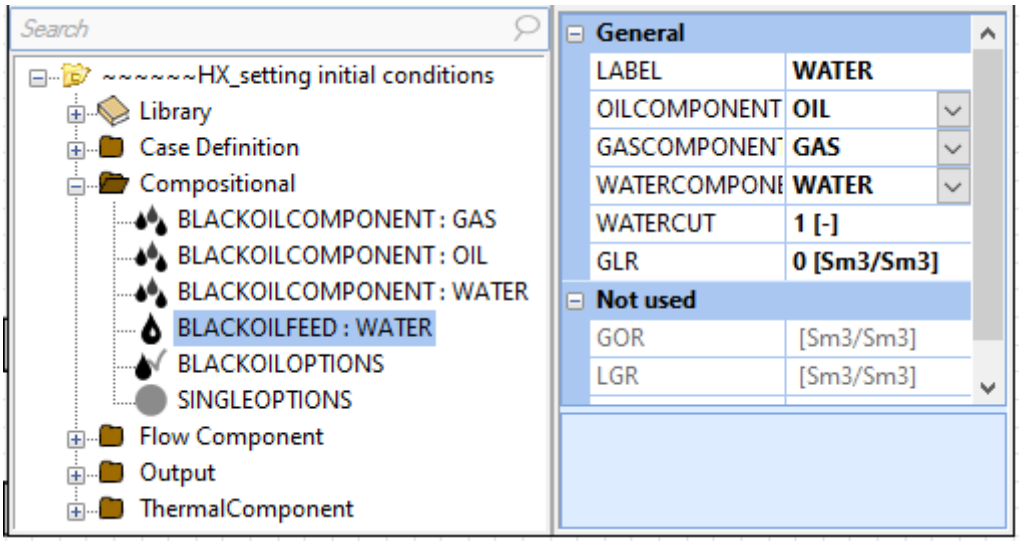

Figure 24: Layout of the "Compositional" folder

Properties of all fluids are input in these areas, but it is not until the next sub-folder “Black Oil Feed: Water” that water is defined as the only phase in this model. In fact, the water-cut is set at a value of 1, which means that the fluid is composed of 100% water.
In addition, the gas liquid ratio (GLR) is set at 0 suggesting no gas in the fluid feed (figure 11).

Succeeding the “Compositional” folder is the “Flow Component” folder. Its layout is depicted in figure 25 below.

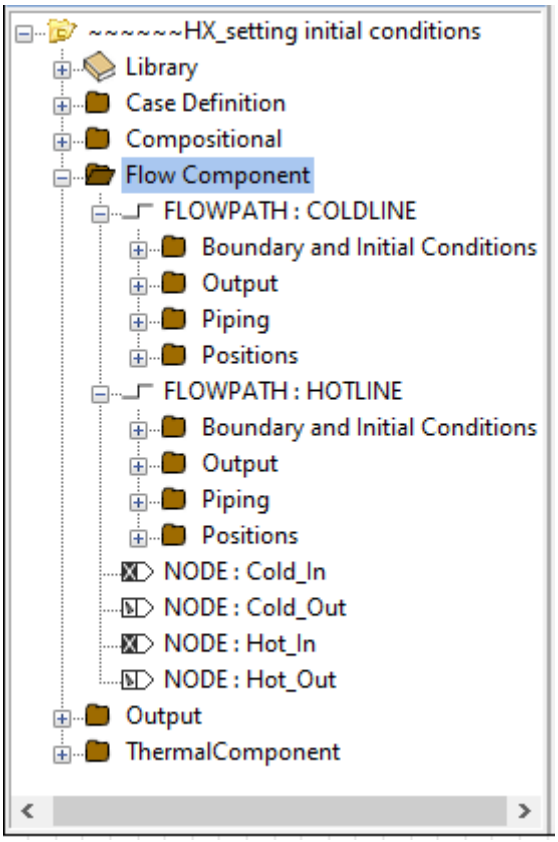

Figure 25: Layout of the "Flow Component" folder

This folder basically deals with objects of the simulation network. Here, two major components are distinguishable: Flow paths and nodes. Flow paths, in terms of simulation, point to the pipes constituting the heat exchanger, and which are responsible for fluid transport. Naturally, there are two separate flow paths: one for each fluid. For each of them, the following sub-folders reside: Boundary and initial conditions, Output, Piping and Positions.

Below is a representation of the “Flow Path” component for the case of the cold fluid:

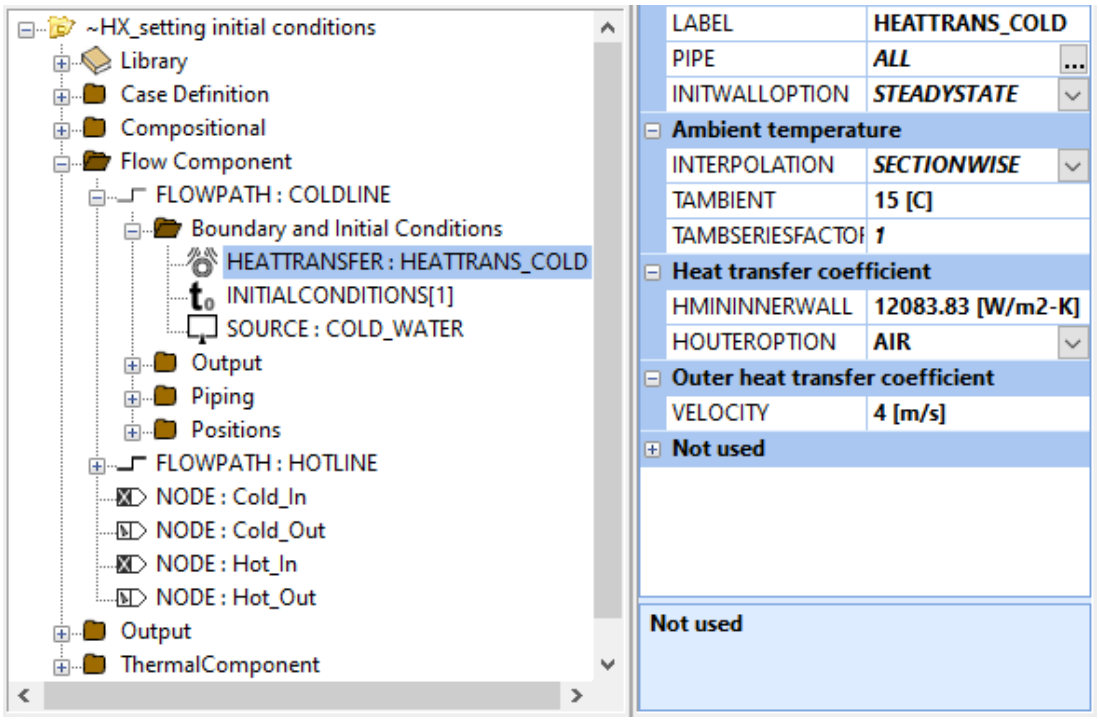

Figure 26: Layout of the "Flow Path" component for the cold fluid

In the “Boundary and Initial Conditions” folder shown in figure 26, factors like ambient temperatures and heat transfer coefficients are dealt with in the “Heat Transfer” section. In this case, ambient temperatures refer to the temperature of the fluid surrounding the fluid in question. So, for the hot fluid, the ambient temperature is that of the cold fluid, while in the case of the latter, the ambient temperature is that of surrounding ambient air in the lab, which is conventionally set at 15°C. Thus, the velocity of the ambient fluid (air) is set to 4 m/s.

As previously mentioned, these conditions are not accounted for in the theoretical calculations, as the ambient air temperature has not been considered. Such conditions may be a source of unalignment between both methods. The reason for disregarding ambient conditions in theoretical application is to eliminate any changes in kinetic and potential energy that may interfere with the fluid in question. This creates an energy balance for each fluid, within a differential section.

This is indeed interpreted as an equality between the rate of heat loss by the hot fluid at any point of the heat exchanger and the rate of heat gain by the cold fluid in the same section. The previous statement is therefore described by the following equations:

$$\partial \dot{Q} = \dot{m}_h c_{p,h} dT_h \qquad \text{(Eq. 23.a)}$$

$$\partial \dot{Q} = \dot{m}_c c_{p,c} dT_c \qquad \text{(Eq. 23.b)}$$

As for the heat transfer coefficients, they are separately input in OLGA based on the values concluded from hand-calculations.

Subsequently under the “Initial Conditions” sub-folder presented in figure 27 below, initial values are stated. This segment intersects with theoretical calculations as they both require the input of fluid temperatures at the inlet.

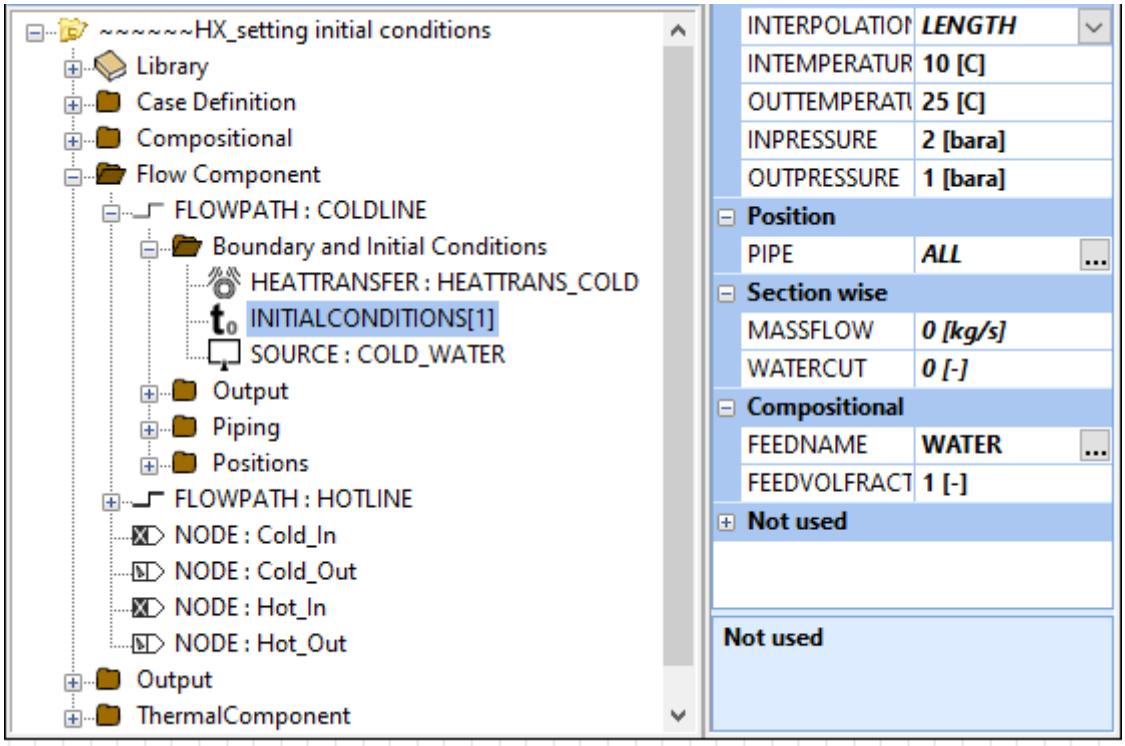

Figure 27: Layout of the "Initial Conditions" sub-folder for the cold fluid

The difference is that OLGA offers a domain to enter outlet temperatures of the two fluids as well, which are otherwise calculated in theory. For that matter, an assumption of these values was made; 25°C each for inlet temperatures of 40°C for the hot water and 10°C for the cold water.

In addition, there is a field for inlet and outlet pressure values. Although e-NTU method calculations do not account for pressure variations, input values in OLGA were based on realistic lab conditions. Particularly 2 bar and 1 bar for the inlet pressure of the cold fluid, and its outlet pressure, respectively. Simultaneously for the hot fluid, pressures are set at 1.5 bar and 2 bar for the inlet pressure and the outlet pressure, respectively.

Additionally, a mass-type source was assigned for both sides of the heat transfer in the “Source” sub-folder. This can be seen in figure 28. Also, temperatures here refer to inlet temperatures because the sources are placed at the inlet, as shown in figure 29 below:

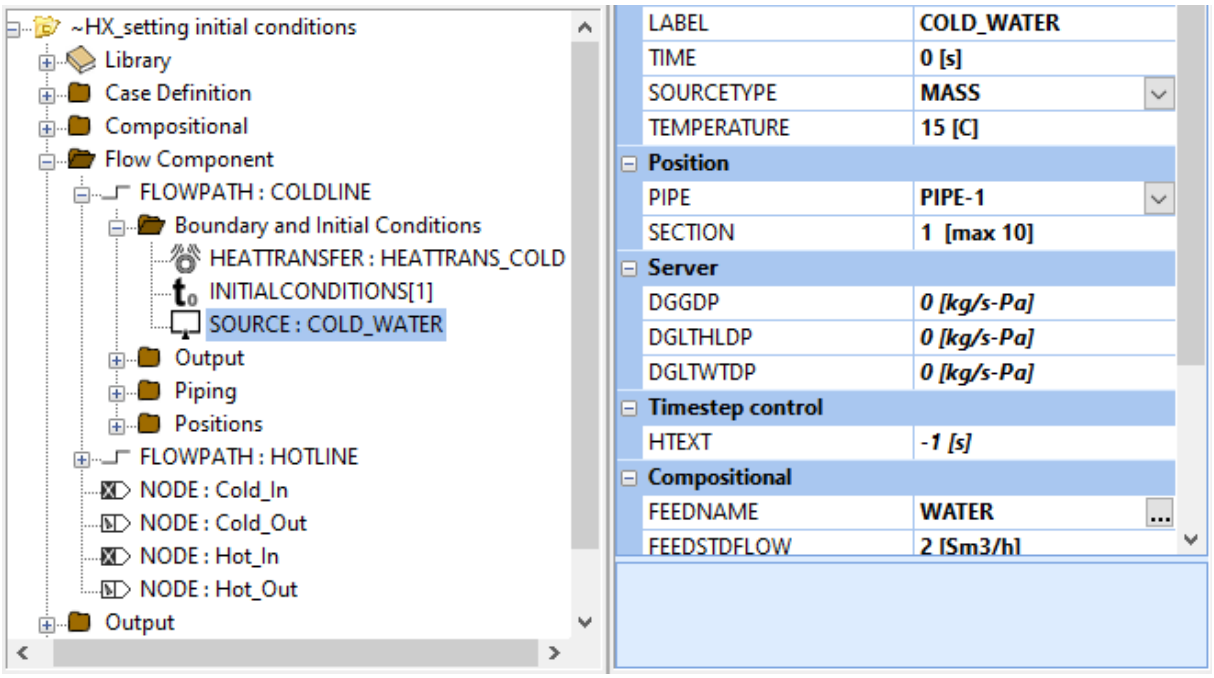

Figure 28: Layout of the "Source" sub-folder for the cold fluid

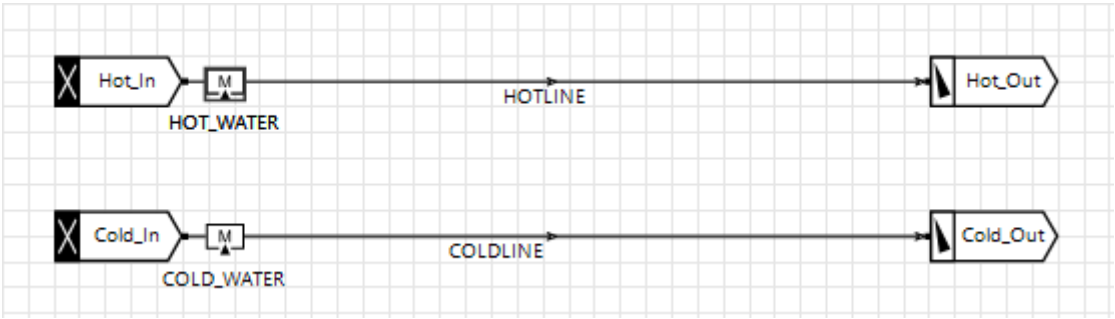

Figure 29: Component Scheme

This is also described in the section number related to the mass source. It dictates the section of the pipe where the source is located, and it takes in this case 1 as value since the sources are in the first section of the streamlines. It is crucial to note here that when attempting to model different cases, values of inlet temperatures should be modified here as well as in the “Initial Conditions” section. At the same time, it is possible now to input the flow rates of both fluids in the “Source”, which are also input parameters in the hand-calculation step.

As for the “Output” sub-folder, it revolves around the parameters to be plotted at the end of the simulation for the starting and ending sections of the flowlines. Here, the parameters in question are rates of heat transfer, temperature and pressure. There are of course many other parameters to choose from, yet the ones previously enumerated are the most relevant to us. A depiction of this sub-folder is found in figure 30 below:

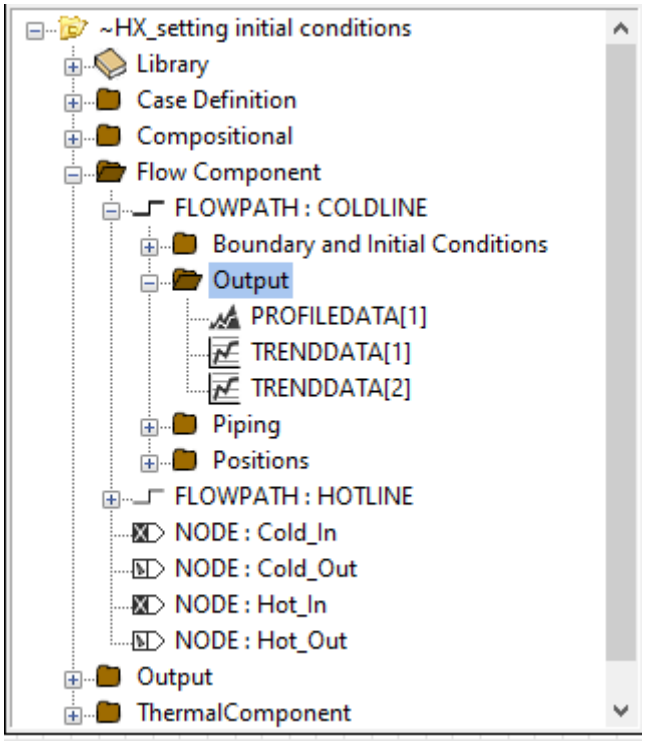

Figure 30: Layout of the "Output" sub-folder for the cold fluid

Moving on to the “Piping” sub-folder seen in figure 31, crucial parameters to be accounted for are the diameter and length of the pipe in addition to its roughness, which is estimated by 10^{-4} mm. Pipe roughness is taken from the steel properties table.

Although pipe thickness has been already input in a previous step, diameters are yet to be defined. This value here suggests outer diameters.

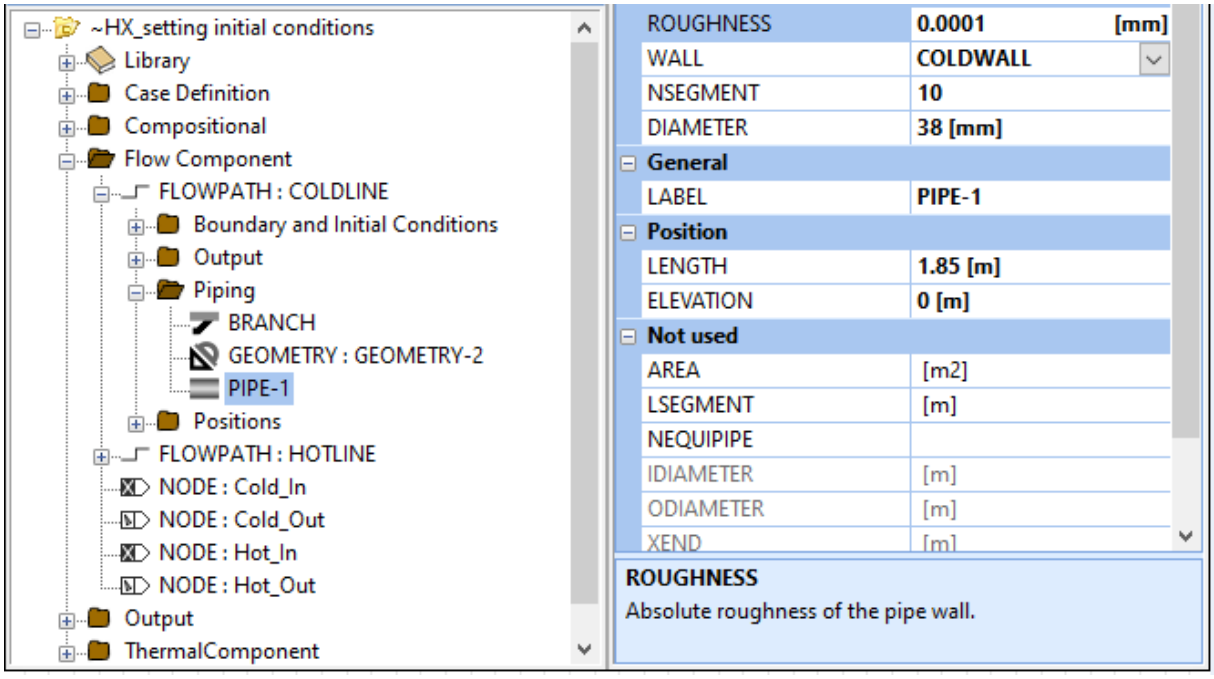

Figure 31: Layout of the "Piping" sub-folder for the cold fluid

As for the pipe length, it can only be plugged in once generated as a result of the e-NTU method. This is in fact where both methods diverge and prevail a validation approach that involves them simultaneously. First, using the e-NTU method, the length of the heat exchanger is calculated. Then, parameters defined in the previous method are plugged in OLGA, followed by the calculated length. Lastly, results of the simulation are compared to those generated in the hand calculations.

With regards to the “Positions” folder, it contains the number of sections into which the simulation is divided, in this case 10. This is laid out in the following figure 32.

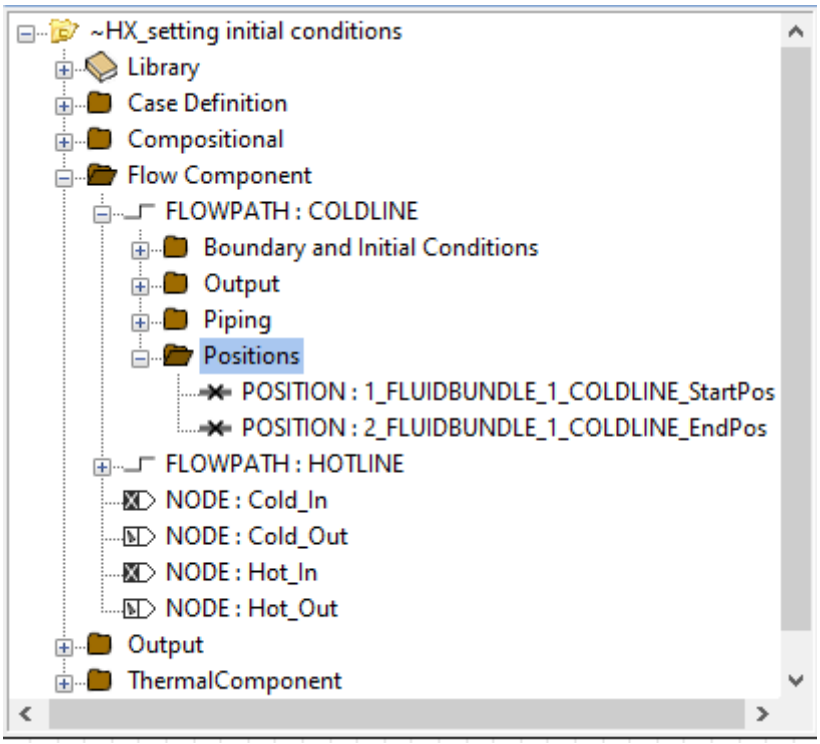

Figure 32: Layout of the "Positions" sub-folder for the cold fluid

As for the different nodes in this bundle, a total of four is used, with two closed nodes at both inlets and two pressure nodes at the outlets where temperatures and pressures need to be defined. This in fact designates inlet temperatures because when given pressures nodes, outlet temperatures are interpolated based on previous inputs.

Moving on to the “Output” folder of the model, plotting and presenting results are dealt with here. The layout of this folder is presented in figure 33.

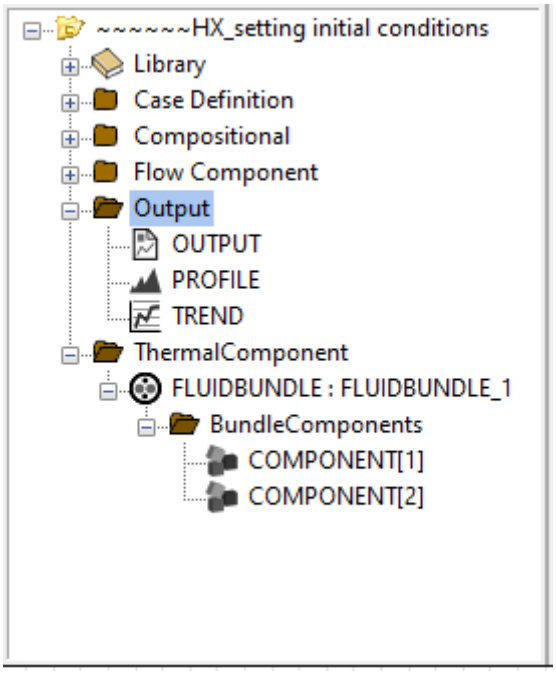

Figure 33: Layout of the "Output" and "Thermal component" folders

After defining general parameters such as number of variable columns, or time interval between output printings, then plotting options are either profiles or trends. The difference is that in profiles, variations of one parameter are showcased through the whole system length, while profiles are a representation of one variable at a specific position versus time.

Lastly, the thermal component: they are represented by a fluid bundle (figure 33) which mimics the positions of the fluid streamlines in relation to each other. This is better shown in figure 34 below:

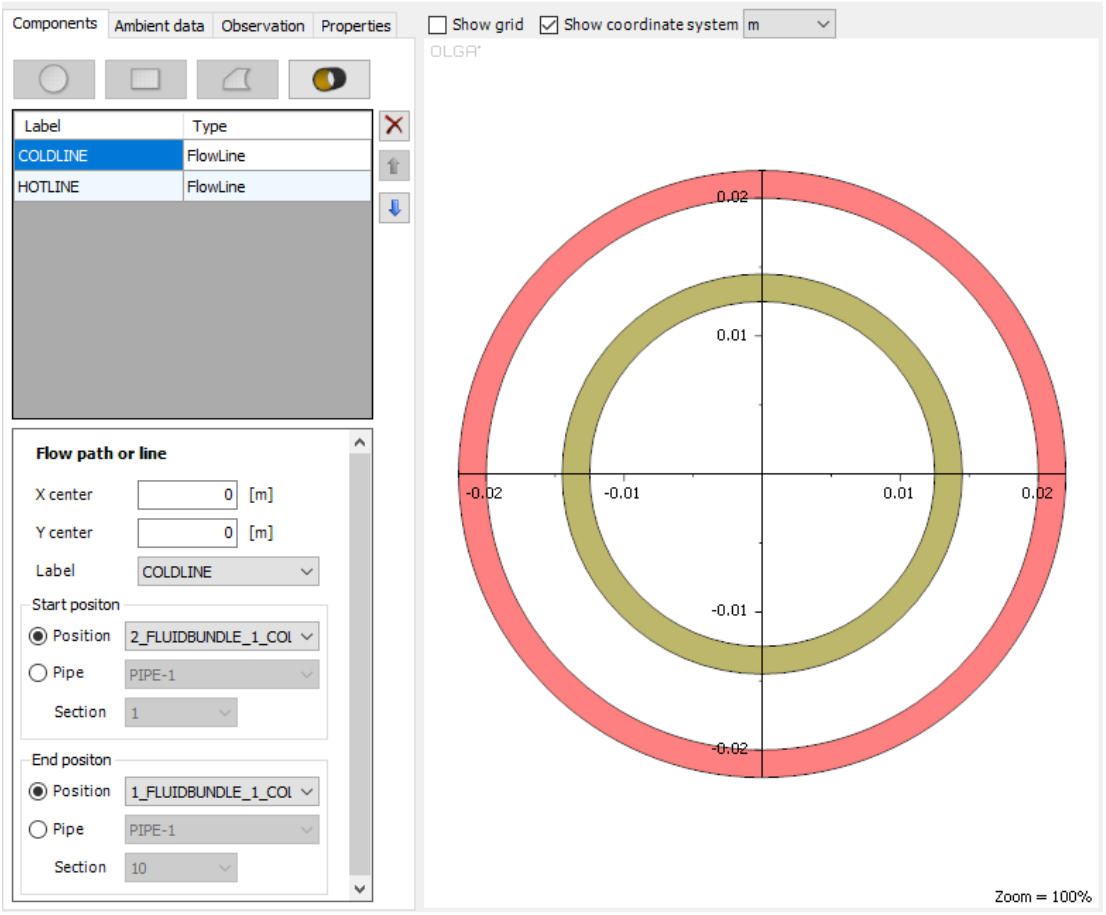

Figure 34: Fluid bundle layout

This in fact resembles a cross-section of the heat exchanger pipes. Figure 34 shows both pipes in a concentric assembly, with the pipe transporting the hot fluid on the inside. Meanwhile, the cold fluid in the outer pipe is surrounded by ambient air, where a fraction of heat transfer occurs.

The previous figure also puts both pipe diameters and thicknesses in display. Both parameters were already input in previous steps but can be displayed here. Diameters presented in this case are 40 mm and 25 mm for the cold and the hot pipes, respectively.

Besides, the counter-flow arrangement of the heat exchanger is ensured by placing inlets at opposite ends of the flow stream. It is translated in OLGA by the number of the section that holds the inlet. As seen in figure 34, the starting position of the cold fluid is at the first section of the pipe, while its ending position is at the tenth (and last) section of the pipe. This also implies that these positions are reversed in the case of the hot fluid since we are dealing with a counter-flow type of construction.

5.3 Adjustments to real lab conditions:

The previous chapter contained a detailed workflow of constructing the OLGA model which serves as a flow simulation in the heat exchanger. However, this model as well as the e-NTU method calculations are the first step of problem solving. In fact, the model is only valid when it generates results that are close-enough to the real case experienced in the pump testing facility.

Nevertheless, a few of the input data described in the previous chapter underwent some alterations along the course of the project. These parameters are described as follows.

- Pressures:

As stated before, inlet pressures of both cold and hot fluid streams were introduced in the OLGA simulation based on real lab test results, since hand-calculations relative to the e-NTU method do not account for pressure values. These pressures were input under the “Initial Conditions” section, and then set at 2 bar and 1 bar for the inlet pressure and the outlet pressure of the cold fluid, respectively. Meanwhile, those of the hot fluid were set at 1.5 bar and 2 bar for the inlet and the outlet, respectively.

- Pipe length:

Due to size limitations imposed at the testing facility, the prime challenge of this design has been to calculate a proper length of the heat exchanger, which conforms to its initial working conditions. Nevertheless, this strategy seems short when taking size restrictions into account. For that matter, a variable sizing method has been developed in order to have flexible heat exchanger lengths with a single design. A display of the pipe arrangement can be seen in the following figure 35, which is taken from the lab.

Figure 35: Pipe arrangement of the HX at the testing facility

In accordance to figure 35, the heat exchanger at the lab is composed of 4 pipes, each with a length of 4.5m. Valves, playing the role of a sealing element, are installed at the end of each pipe section and depending on their closed or open status, they control the length of the pipe. This feature not only provides a flexible design, but also increases the operating options of the heat exchanger.

During comparison of the results between the e-NTU method and the simulation, the heat exchanger length was considered 9m. This translates to 2 active pipe sections, and the simulation was made accordingly.

- Pipe diameters:

Although pipe dimeters were initially set to be input by the user as initial parameters, they are now fixed in the simulation at constant values of 38cm and 30cm for both outer dimeters of the cold and the hot fluid streams, respectively. The wall thicknesses being 2mm for each case, this leaves us with inner diameters of 34cm and 26cm for the cold and the hot fluid streams, respectively. Therefore, simulations are now run using constant values of pipe diameters.

- Maximum fluid flow rates:

Initially, as fluid flow rates were introduced, they were in the range of 5 m^3/h and 20 m^3/h for the hot fluid, meanwhile, that of the cold fluid is less than 2 m^3/h. That, in fact, raised issues in the simulation despite being completely valid from a theoretical point of view. In OLGA, results showed very minor changes in the temperature of the hot fluid, meaning that a heat transfer between it and the cold fluid barely occurred. This is translated by a very small difference in temperature of the hot fluid between its outlet and its inlet.

An immediate observation was that the big difference in flow rates between the two fluids probably plays a factor. In simple terms, this may mean that since the hot fluid travels at relatively higher rates compared to the cold one, the former is not in contact with the cooling source long enough for a thorough heat transfer to take place.

In practice, this was mitigated by reducing the range of flow rate for both fluids. In fact, those of the hot fluid are now at a maximum of 5 m^3/h, while flow rates of the cold fluid are ranging below 0.9 m^3/h. Once this change has been implemented, more meaningful results were seen. This can be explained by reducing the difference in the range of flow rates.

6 Result Comparison

In this chapter, the methods used to compare results are discussed. After conducting theoretical hand-calculations as well as a multiphase simulation, it is important to compare these two methods to one another, as well as to the results of the lab tests. These results may show alignment or differences, which in turn can shed the lights on their accuracy or on possible factors crucial to the design of the heat exchanger.

6.1 Comparing e-NTU to OLGA

As discussed in Chapter 5, the effectiveness-NTU method was used for the design of this heat exchanger, since it obeys the requirements of our working conditions. Indeed, it is a method best used when the type of heat exchanger is known and when determining the efficiency and the performance of a given heat exchanger, namely its heat transfer rate and its outlet temperatures.

Although the goal of the design was initially intended to determine the size of the heat exchanger that will accomplish a given rate of heat transfer, making the LMTD method sound like better candidate for the task, yet the absence of the outlet temperatures on one hand and the overall heat transfer coefficient on the other hand make it difficult to conclude the heat transfer rate from an energy balance. Therefore, this still confirms the e-NTU method as more eligible. [1]

Fundamentally, the validation method consists of implementing in OLGA the initial conditions that have been considered for the e-NTU calculations. The following step would be to run the simulation and compare the outcome results with those procured by hand-calculations. The aim of this task is to confirm whether the results of both methods affiliate, and if not, to try to extract an explanation.

The input variables from the e-NTU method calculations are summarized in the figure below.

				Inner pipe		Outer pipe					Ui	Uo
Q̇ [kw]	qc [m³/h]	qh [m³/h]	Th, in [°C]	Di [m]	Do [m]	Di [m]	Do [m]	L [m]	Th, out [°C]	Tc, out [°C]	[W/m²K]	[W/m²K]
15	0.7	3	40	0.026	0.03	0.034	0.038	5.60767767	35.6979902	33.4371848	2661.0867	2306.27514

Figure 36: Variable guide of the e-NTU method

As shown in figure 36, the following parameters are considered as input data, and serve to feed the e-NTU calculation process: heat transfer rate, flow rate of the cold fluid, flow rate of the hot fluid, inlet temperature of the hot fluid and lastly, inner as well as outer diameters of both pipes. Note that the inlet temperature of the cold fluid is also an input parameter, of constant value. It has been implemented in earlier stages of the calculations, that is why it is not showcased in the figure above.

Meanwhile, on the right side of the table, the calculated parameters are marked in red. They are indeed the length of the heat exchanger and its outlet temperatures.

Still, a slight change in the format of the design occurred. In fact, the heat transfer rate that was once considered an input parameter is no longer to be input. However, it is now rather used as a transitional parameter which will help to calculate the outlet temperatures as well as the size of the heat exchanger using a reverse-calculating method.

This coincides with the fact that the input of the heat transfer rate in OLGA is not an option, as the software interface does not offer this field. This can easily lead to a lot of nuances in the results, because in the hand-calculations for example, maintaining all the input parameters intact while only changing the heat transfer rate will result in different outcomes regarding the length and the outlet temperatures of the heat exchanger. By the same token, since OLGA does not account for the heat transfer rate as an input, the results of its simulation will show only one of the many possible outcomes for the chosen combination of values.

While calculations based on the e-NTU method generate the desired output parameters, OLGA portrays its results using the “Trend” section, in the form of a curve plotted versus pipe length.

It is important here to note that although results simulated by OLGA are plotted throughout the entire length of the pipe, only the values shown at the full length of the pipe are of significance to the design. As a matter of fact, outlet temperatures of either fluid refer to temperatures at which the fluid exits the heat exchanger, which in practical terms refers to the whole length of the pipe.

It is also important to mention that not only do the simulated results depend on pipe length, but they are also bound to the duration of the simulation. This means that simulated results are only meaningful once the simulation is conducted to its full extent. In this case, a simulation period of 60 seconds has been placed.

Moreover, applying adjustments to real lab conditions discussed in chapter 5, gave way to several invalid cases upon input in Excel. These cases were revealed through trial and error, which then enabled to sieve valid working cases such as the one portrayed in figure 36 above. The results of these working cases were then matched with the ones generated by OLGA using the validation method.

Despite many invalid cases, the comparison conducted between the e-NTU method and the OLGA simulation still showed a high degree of convergence especially with regards to the outlet temperatures. And although some disparities were seen in the overall heat transfer coefficient values, they are almost negligeable, and only reflect the instable nature of this parameter as it is highly sensitive to temperature and thermal resistance.

Below are the results generated by OLGA corresponding to the data from figure 36:

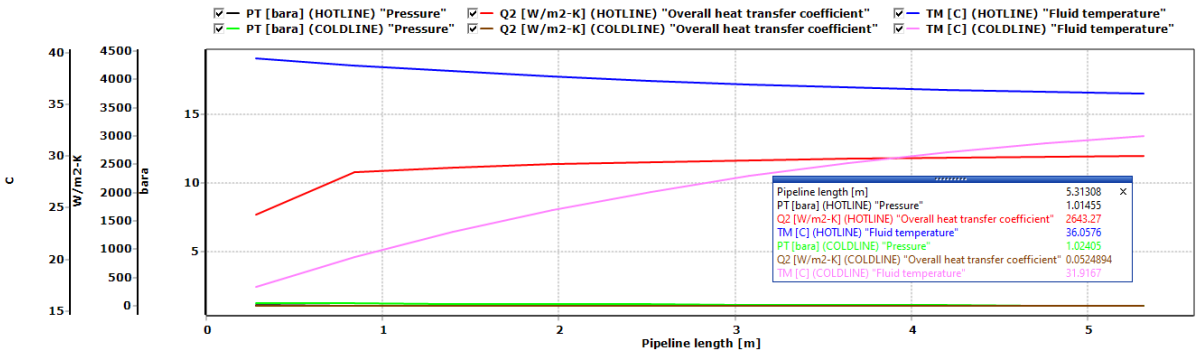

Figure 37: Comparing simulation results to e-NTU.

Comparing both methods shown in figures 36 and 37, it is possible to conclude their alignment. As a matter of fact, the overall heat transfer coefficient calculated via the e-NTU method is estimated by 2661.08 W/m²K, versus 2643.27 W/m²K in OLGA. Regarding outlet temperatures, the e-NTU method predicted 35.69 °C for the hot fluid and 33.43 °C for the cold fluid, meanwhile in OLGA, these values are 36.06 °C and 31.9 °C with respect to the hot and cold fluids.

A series of other cases of comparison was conducted under the same conditions. They are summarized in the table below.

Table 3: Summary of e-NTU VS OLGA results

	$T_{h,\,out}$ [°C]		$T_{c,\,out}$ [°C]		U [W/m²K]	
	e-NTU	OLGA	e-NTU	OLGA	e-NTU	OLGA
Case 1	38.92	37.88	36.51	37.49	742.84	1543.52
Case 2	35.69	36.06	33.43	31.9	2661.08	2643.27
Case 3	29.39	31.62	24.56	24.25	1733.59	1830.59
Case 4	39.13	39.19	22.17	21.67	2810.94	2552.95
Case 5	37.84	37.9	22.17	21.95	2173.08	2049.92
Total Average	± 0.75		± 0.7		± 259.328	

Table 3 showcases the variation in the results given by both the e-NTU method and the simulation. These variations are rather slight, and results show an overall convergence, illustrated by the “Total Average” values. These values are absolute and are calculated as an average in difference of all five batches of comparisons shown in the previous table. For each parameter, the “Total Average” reflects the degree to which both methods align. For example, in the case of the outlet temperature, the simulation is likely to predict the same results calculated using the e-NTU method with a precision of ± 0.75 °C.

6.2 Comparing testing Facility to OLGA

Due to the slight modification that has struck a chord in the workflow of the design, the prime focus has shifted from the size and length of the heat exchanger to its efficiency and performance in terms of heat transfer. This means that the most important parameters to

look after are now the outlet temperatures of the system, in addition to the overall heat transfer coefficient of the heat exchanger. [2]

Therefore, an alternative validation workflow was used in order to calculate the heat transfer coefficient and therefore conclude the physical properties of the hot fluid, namely its flow rate. It is what has been earlier described as the reverse-calculation method.
This principle is based on the following equation, which is derived from the first principle of thermodynamics.

$$\dot{Q} = C.\Delta T = C_c \left(T_{c,out} - T_{c,in}\right) = C_h \left(T_{h,in} - T_{h,out}\right) \quad \text{(Eq. 26)}$$

Inlet and outlet temperatures of both fluids, as well the flow rate of the cold fluid, are taken from real lab tests, while the capacity rate of the cold fluid C_c is calculated using its mass flow rate and the heat capacity of water, according to (Eq.3), described in chapter 5. From there, it is possible to calculate the heat transfer rate. This will in turn allow us to conclude the flow rate of the hot fluid which can later be input in OLGA as an initial variable.

Below, a comparison of the two methods is displayed via screenshots. As mentioned above, the parameters to be assessed are the outlet temperatures and the overall heat transfer coefficient, with emphasis on the hot fluid. This is since the entire study revolves around cooling the hot water by redirecting it through a heat exchanger.

First up is the reverse-calculation method. Its results are summarized in the figure below:

	qc [m³/h]	Tc, in [°C]	Tc, out [°C]	Th, in [°C]	Th, out [°C]	Q̇ [kw]	qh [m³/h]	hi [W/m²K]	ho [W/m²K]	Ui [W/m²K]	Uo [W/m²K]
case1	0.25	14.6	37.8	38.8	35.72	6.741035	1.883117	4749.92	754.9	693.8	601.32
case2	0.59	13.02	34.3	38.43	30.17	14.59225	1.52	4749.92	5184.23	2172.1	1882.5
case3	0.7	12.7	31.03	38.37	26.87	14.9128	1.115739	2597.37	5554.9	1603.32	1389.55
case4	0.89	12.52	36.07	38.31	27.1	24.36013	1.869715	4749.92	7170.63	2415.03	2093.02
case5	0.94	12.58	30.95	38.6	26.92	20.06946	1.478408	2597.37	7170.63	1699.09	1472.55
case6	0.31	13.14	38.03	38.74	34.75	8.967785	1.93381	4749.92	754.9	693.84	601.32

Figure 38: Summary of the results of the reverse-calculation method

Figure 38 exhibits the results of 6 separate case studies. As mentioned before, these results are based on actual lab test recordings, with a light collaboration with theoretical calculations. Based on that, it is easy to distinguish 3 main compartments within figure 38.

The first compartment situated on the left side of the figure deals with actual lab values. At the same time, it plays the role of input data in OLGA as explained before. These values were then used to conclude the heat transfer rate of the heat exchanger, and from which we can compute the flow rate of the hot fluid. Both these parameters are displayed in the middle compartment of figure 38.

In conjunction, the right side of the table shows the heat transfer coefficients for the hot and cold fluids respectively, and the overall heat transfer coefficients with respect to the inside and outside surface areas of the pipes. Both parameters, corresponding to each case, were calculated in previous stages using the e-NTU method. They are then displayed in this

fashion to make comparison matters easier. Results of the simulation can hence be introduced.

In order to generate the following results, simulations were conducted under two different environments: an insulated system and a non-insulated system. Although insulation mimics perfectly the theoretical aspect of the calculations using the e-NTU method, neglecting it reflects a more realistic vision of the heat transfer that takes place in the facility. Hence, simulation results under non-insulated conditions are used in the comparison below. Nevertheless, we can note that both conditions showed very minor differences in the results. The product of the simulation under insulated conditions are displayed in the appendix.

Meanwhile, comparisons below are done with reference to figure 38.

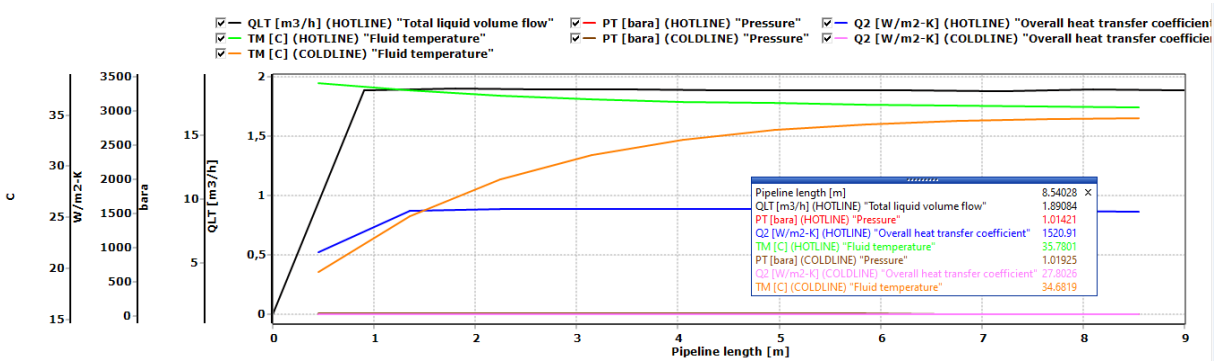

Figure 39: Case 1 of simulation results

This first case of simulation lays out a precision with regards to the outlet temperature of the hot fluid. In fact, it shows a value of 35.78°C versus 35.72 in theory. It also shows very similar values of flow rate with 1.89 m^3/h versus 1.88 m^3/h in theory. As for the overall heat transfer coefficient on the hot fluid's end, results did not match, as the simulation showed 1520.9 W/m²K, versus 693.8 W/m²K in theory.

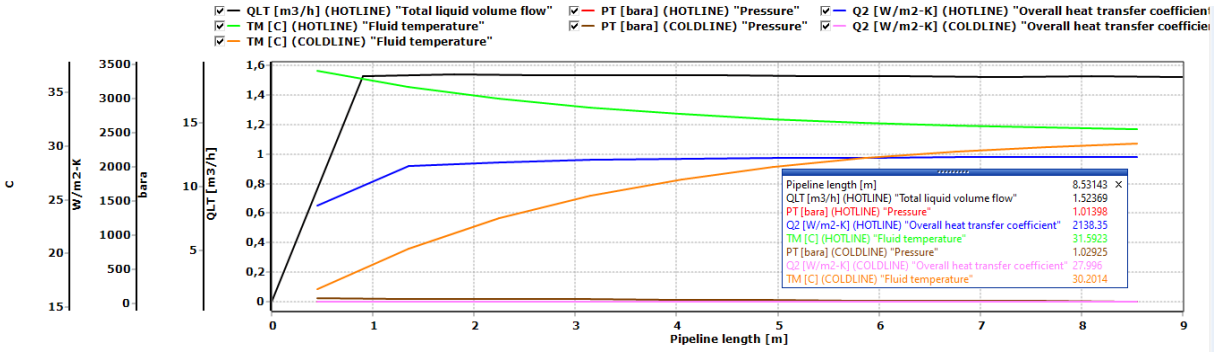

Figure 40: Case 2 of simulation results

This second case of simulation displays a precision with regards to the outlet temperature of the hot fluid. In fact, it shows a value of 31.59°C versus 30.17 in theory. It also shows identical values of flow rate with 1.52 m^3/h on both ends. Moreover, overall heat transfer

coefficients are very similar, as the simulation showed 2138.35 W/m²K, versus 2172.1 W/m²K in theory.

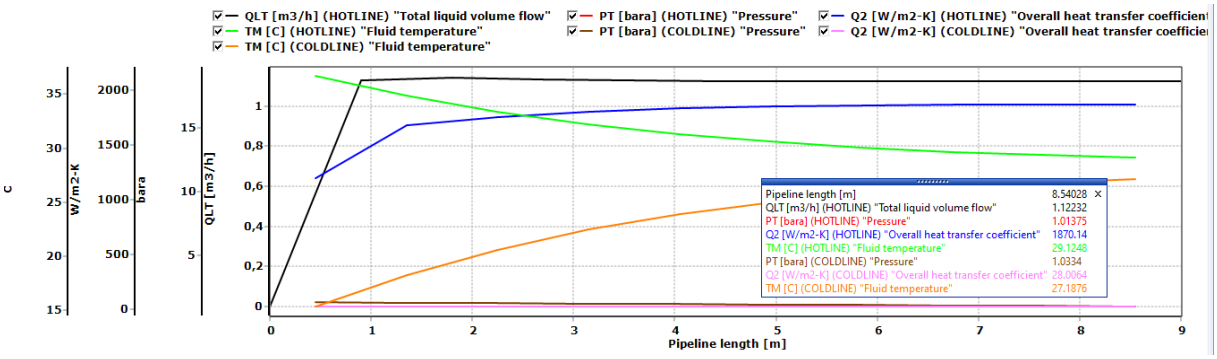

Figure 41: Case 3 of simulation results

The third case of simulation demonstrates a slight refraction regarding the outlet temperature of the hot fluid. In fact, it shows a value of 29.12°C versus 26.87 in theory. It also shows very similar values of flow rate with 1.12 m^3/h versus 1.11 m^3/h in theory. While in the case of the overall heat transfer coefficient, results are close since the simulation showed 1870.14 W/m²K, versus 1603.32 W/m²K in theory.

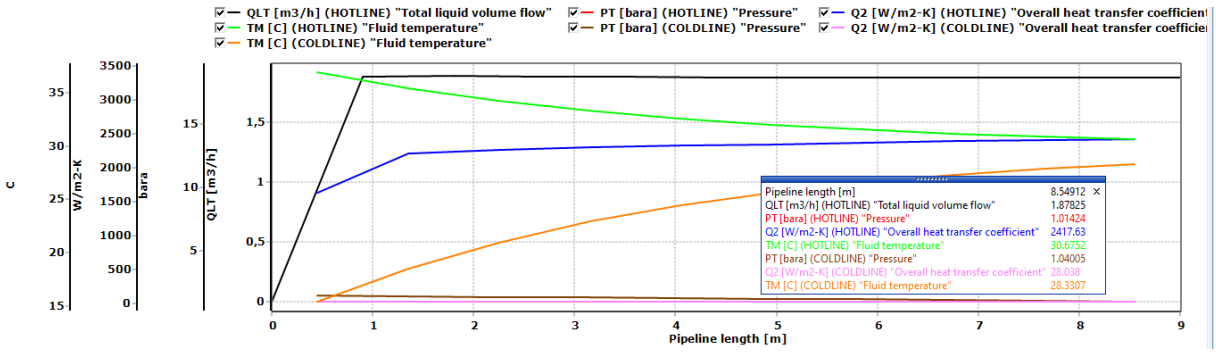

Figure 42: Case 4 of simulation results

This fourth case of simulation displays a small difference with regards to the outlet temperature of the hot fluid. In fact, it shows a value of 30.67°C versus 27.1 in theory. It also shows almost identical values of flow rate with 1.87 m^3/h versus 1.869 m^3/h in theory. The same goes for the overall heat transfer coefficients, as the simulation showed 2417.63 W/m²K, versus 2415.03 W/m²K in theory.

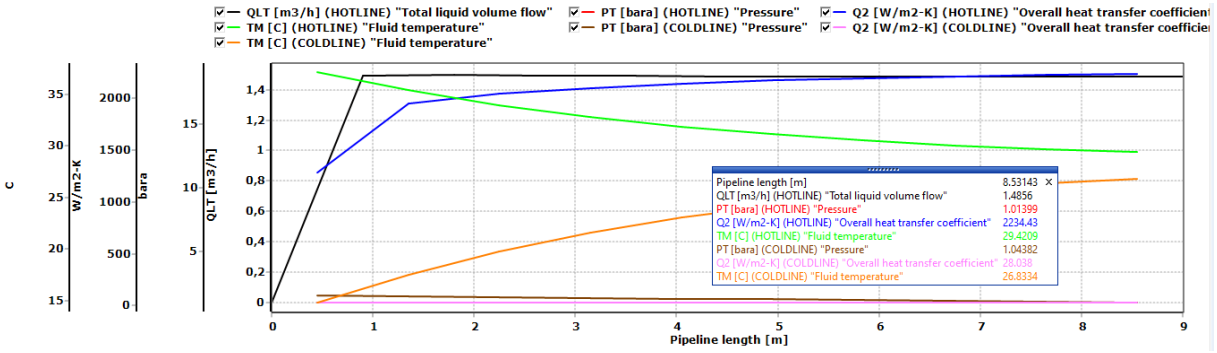

Figure 43: Case 5 of simulation results

The fifth case of simulation presents a difference regarding the outlet temperature of the hot fluid. In fact, it shows a value of 29.42°C versus 26.92 in theory. It also shows very similar values of flow rate with 1.48 m^3/h versus 1.47 m^3/h in theory. While in the case of the overall heat transfer coefficient, results are slightly diverged since the simulation showed 2234.4 W/m²K, versus 1699.09 W/m²K in theory.

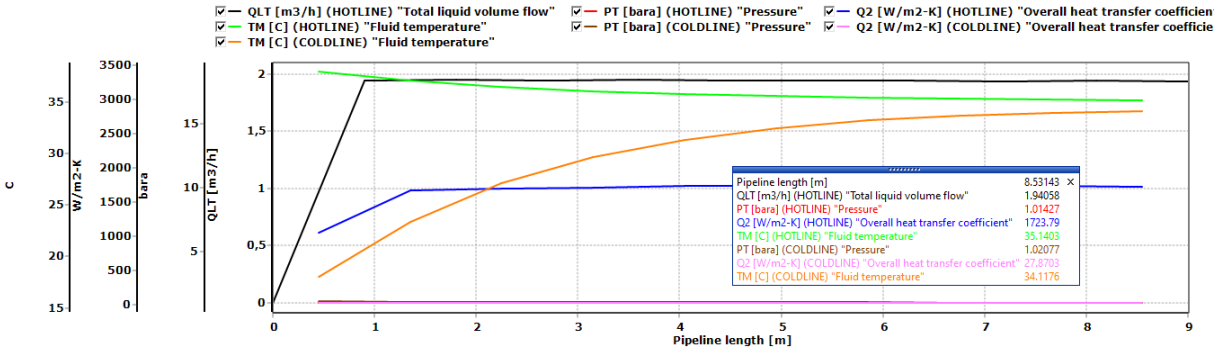

Figure 44: Case 6 of simulation results

This sixth case of simulation reveals a small difference with regards to the outlet temperature of the hot fluid. In fact, it shows a value of 35.14°C versus 34.75 in theory. It also shows nearly identical values of flow rate with 1.94 m^3/h versus 1.93 m^3/h in theory. In contrast, in the case of overall heat transfer coefficients, the simulation showed 1723.79 W/m²K, versus 693.84 W/m²K in theory.

In the meantime, despite the few differences showcased in the results of the insulated simulation, they are not significant enough to create an impact.

Although values of heat transfer coefficient remain almost intact with or without adding insulation to the system, the difference appears to reside in the outlet temperature of the hot fluid. Though, these nuances in temperature are not impactful as previously noted.
These results are summarized in the table below:

Table 4: Summary of outlet temperature values for different conditions

	$T_{h,\,out}$ [°C], testing facility	$T_{h,\,out}$ [°C], insulated simulation	$T_{h,\,out}$ [°C], non-insulated simulation
Case 1	35.72	36.03	35.78
Case 2	30.17	31.67	31.59
Case 3	26.87	29.18	29.12
Case 4	27.1	30.72	30.67
Case 5	26.92	29.45	29.42
Case 6	34.75	35.3	35.14

6.3 Comparing e-NTU method to testing facility

This second round of comparisons aims to seek how close facility test recordings are to pure theoretical calculations. The latter are based on the e-NTU method which was described in chapter 5. These calculations are not influenced by any assumptions, but rather a straightforward application of the e-NTU workflow.

Once again, the comparison is done with reference to the results displayed in figure 38. Note that the target of this comparison is only the outlet temperature of the hot fluid. As a matter of fact, values of overall heat transfer coefficients are identical to those presented in the previous batch. This is because during the comparison between lab results and simulation results, the calculated overall heat transfer coefficients for each case were stemming from a theoretical approach: the same theoretical approach applied in the following set of results.

				Inner pipe		Outer pipe					Ui	Uo
Q̇ [kw]	qc [m³/h]	qh [m³/h]	Th, in [°C]	Di [m]	Do [m]	Di [m]	Do [m]	L [m]	Th, out [°C]	Tc, out [°C]	[W/m²K]	[W/m²K]
7	0.3	2	39	0.026	0.03	0.034	0.038	11.5713099	35.9885932	34.6760456	693.839062	601.327187

Figure 45: Case 1 of e-NTU method results

The first case shows an outlet temperature of 35.98°C for the hot fluid, while that recorded in the test facility is 35.72°C. The difference here is negligeable, confirming an alignment between both methods of calculation.

				Inner pipe		Outer pipe					Ui	Uo
Q̇ [kw]	qc [m³/h]	qh [m³/h]	Th, in [°C]	Di [m]	Do [m]	Di [m]	Do [m]	L [m]	Th, out [°C]	Tc, out [°C]	[W/m²K]	[W/m²K]
15	0.6	2	38	0.026	0.03	0.034	0.038	9.40558835	31.5469853	34.5300489	2172.10201	1882.48841

Figure 46: Case 2 of e-NTU method results

This case shows an outlet temperature of 31.54°C for the hot fluid, while that recorded in the test facility is 30.17°C. The difference is relatively small.

				Inner pipe		Outer pipe					Ui	Uo
Q̇ [kw]	qc [m³/h]	qh [m³/h]	Th, in [°C]	Di [m]	Do [m]	Di [m]	Do [m]	L [m]	Th, out [°C]	Tc, out [°C]	[W/m²K]	[W/m²K]
15	0.7	1	38	0.026	0.03	0.034	0.038	12.2401113	25.0939707	31.1371848	1603.32722	1389.55025

Figure 47: Case 3 of e-NTU method results

The third case shows an outlet temperature of 25.09°C for the hot fluid, while that recorded in the test facility is 26.87°C. The difference here is also small.

				Inner pipe		Outer pipe					Ui	Uo
Q̇ [kw]	qc [m³/h]	qh [m³/h]	Th, in [°C]	Di [m]	Do [m]	Di [m]	Do [m]	L [m]	Th, out [°C]	Tc, out [°C]	[W/m²K]	[W/m²K]
25	0.9	2	38	0.026	0.03	0.034	0.038	21.5207181	27.2449756	36.4200543	2415.03107	2093.02693

Figure 48: Case 4 of e-NTU method results

The fourth case exhibits an outlet temperature of 27.24°C for the hot fluid, while that recorded in the lab is 27.1°C. This case also highlights a negligeable difference.

				Inner pipe		Outer pipe					Ui	Uo
Q̇ [kw]	qc [m³/h]	qh [m³/h]	Th, in [°C]	Di [m]	Do [m]	Di [m]	Do [m]	L [m]	Th, out [°C]	Tc, out [°C]	[W/m²K]	[W/m²K]
20	0.9	1	39	0.026	0.03	0.034	0.038	17.7344797	21.7919609	31.7000435	1679.86072	1455.87929

Figure 49: Case 5 of e-NTU method results

The fifth case reveals an outlet temperature of 21.79°C for the hot fluid. Meanwhile, that recorded in the test facility is 26.92°C. In this case, the difference between both temperatures is large, reaching 5.13°C.

				Inner pipe		Outer pipe					Ui	Uo
Q̇ [kw]	qc [m³/h]	qh [m³/h]	Th, in [°C]	Di [m]	Do [m]	Di [m]	Do [m]	L [m]	Th, out [°C]	Tc, out [°C]	[W/m²K]	[W/m²K]
9	0.3	2	39	0.026	0.03	0.034	0.038	44.3565506	35.1281912	38.9520587	693.839062	601.327187

Figure 50: Case 6 of e-NTU method results

The sixth case presents an outlet temperature of 35.12°C for the hot fluid, while that recorded in the lab is 34.75°C, which also accounts for a very negligeable difference.

At first glance, results derived from the e-NTU method alone are more in harmony with values recorded at the testing facility than results simulated by OLGA.

The temperature difference for each set of compared values is summarized in the table below. Note that these differences in temperature are marked in absolute value.

Table 5: Summary of the difference in outlet temperature for two cases of comparison

	ΔT [°C] Comparing lab and simulation	**ΔT** [°C] Comparing lab and e-NTU
Case 1	0.06	0.26
Case 2	1.42	1.37
Case 3	2.25	1.78
Case 4	3.57	0.14
Case 5	2.5	5.13
Case 6	0.39	0.37
Total Average	± 1.69 °C	± 1.5 °C

The numbers shown in the table above confirm the better alignment of lab results with calculations generated by the e-NTU method solely.

This side-by-side comparison is done between two separate sets of data. On one hand, it is executed by simply calculating the difference in the outlet temperature of the hot fluid between the value recorded at the lab and that generated by the OLGA simulation. On the other hand, the same calculation is realized between the value recorded at the lab and that given by the e-NTU method. This intends to show how close (or far) the predicted results are from the actual ones.

Finally, a total average value is concluded, enabling us to quantify the accuracy of both methods. In this case for example, the simulation is likely to predict results with a tolerance of ± 1.69 °C. Despite the small nuance between the "total average" values of both methods, it is still a good precursor when looking to predict the performance of the heat exchanger.

6.4 Interpretations

The results of comparison which were presented in the previous chapter showed an overall convergence in terms of heat exchanger performance. Yet, looking in detail, a small difference in the calculations can be distinguished. This difference involves the outlet temperatures and resides between the results of using the e-NTU method alone, and results procured by the OLGA simulation when both are directly compared to actual test results from the facility.

The comparison, in fact, showed that lab test results are predicted more precisely using the e-NTU method, versus a multiphase simulation. This is probably due to the complex nature of OLGA, and its reliance on a multitude of algorithms in order to procure precise simulation results. These algorithms may include those of flow assurance such as turbulence and slug modelling, those of fluid composition such as black oil models and Gas/Oli ratio models, or even those of different file data bases like rheology, PVT, compressors and hydrates to name a few. In addition, the software relies on many iterations to execute its calculations. Meanwhile, in this simple heat exchanger model, most of the previously mentioned features are irrelevant, which might be behind the slight divergence of the end results.

On the other hand, results of overall heat transfer coefficients showed mostly accurate predictions, with two out of a total six cases manifesting very different values. An attempt to find the root of this issue lead to a couple of sources citing that the heat transfer coefficient, and therefore the overall heat transfer coefficient, can be among the most difficult parameters to predict in heat transfer. This is due to its uncertainty. In fact, it is highly sensitive to temperature and to thermal resistance. Both factors are almost inevitable when dealing with a heat exchanger. Thermal resistance alterations are very common along pipe walls, where fluid/wall interactions make the wall surface prone to material depositions that could stem from fluid impurities. In addition, many algorithms include radiation effects in heat transfer coefficients when dealing with heat exchangers. [1] [2]

Other factors accentuating the nuance between results may be while inputting data in Excel. This can be noticed when examining figures from the previous chapter, where data input is usually subject to approximations. In fact, values of flow rates, heat transfer rates or temperatures are often rounded to the closest integer value.

This is due to simplification of results on one hand. Since we are already dealing with a large range of input values, it is convenient to raise the increment of passage from one value to another. And on the other hand, it is usually complicated to assign a control with a decimal increment to Excel cells. For that matter, values of results are often referred to a higher integer if their decimal part is equal to or greater than 0.5. This validates even further the idea that the contrast between results originates from the heat transfer coefficient's high sensitivity to temperature. Another factor influencing the precision of the results can be the averaging of thermal properties. This is especially seen with the specific heat of the fluid c_p treated in chapter 4, where an average value of c_p was used for the calculations to reduce the pool of input parameters.

Additionally, the inaccuracy of a few analytical methods is undeniable. This is the case for a few analytical equations that were used for this design during hand-calculations. An example of this is the Nusselt number calculation used in (Eq.12), as well as equations 8.a and 8.b used to conclude a relation for NTU calculation.

7 Summary and recommendations

Starting off this design procedure, the main goal of the study was to design a proper heat exchanger with specific dimensions, which will be able to accomplish a certain heat transfer rate between the hot and the cold fluid. Due to a slight modification to the purpose of this heat exchanger, changes also followed in the workflow and the core structure of the design packages.

As a matter of fact, predicting the performance of the heat exchanger, translated by its outlet temperatures and its heat transfer coefficients, has become of higher priority. This is because we are now dealing with a well-known type of heat exchanger arrangement, along with a specific size, therefore it is no longer a question of structural design, but rather one of efficiency.

It is undeniable that this shift in the end-goal also resulted in a shift in the strategy applied to the task. Initially, a basic and straight-forward effectiveness-NTU method was applied in order to conclude the dimensions of the heat exchanger. Yet, after numerous lab tests have been conducted, it not only reinforced a “data-base” of real cases contributing to the design, but it also modified the design procedure. This is mainly because what was originally considered a given input parameter, now became a parameter to be calculated. The latter being the heat transfer rate $\dot{Q}$.

As a result, a combination of two methods was opted for. It basically consists of a back-calculation of the heat transfer rate, based on actual lab test results. This enables to conclude the physical properties of the hot fluid. From there on, the e-NTU method can be applied again. At this point, the latter is crucial for determining values of effectiveness, heat transfer coefficient, overall heat transfer coefficient and thermal wall resistance.

These calculations were then coupled with a multiphase flow simulation using OLGA, in the aim of reaching matching or converging results. For that matter, the focus will be set on outlet temperatures as well as overall heat transfer coefficients in order to assess the efficiency of the heat exchanger,.

This study was designed to start a new field of research and to open horizons for improving, and even perfecting the concluded results. This tails the fact that primary findings are acceptable yet have a lot of room for improvement.

One way of going about that is by conducting as many tests as possible in the facility. The idea is to further enlarge one’s pool of data in order to maximize options for improvement, and perhaps to couple it with a database constructed specifically to record results in real time and help detect patterns in the functioning of the heat exchanger. More tests conducted will only enrich the database, as well as contribute to an easier prediction of performance in the future.

Another way aiming to improve the outcome of OLGA simulations is to provide a more accurate set of input data. Procuring more detailed parameters to be input in the software will only upgrade the results and shift them closer to real lab results. This englobes ambient air temperatures, fluid pressures, steel properties of the pipes and even the duration of the simulation.

References

[1] Yunus A. Çengel, and Afshin Jahanshahi Ghajar. Heat and Mass Transfer: Fundamentals & Applications. McGraw Hill Education, 2015.

[2] Theodore L. Bergman, Adrienne S. Lavine, Frank P. Incorpera, David P. Dewitt, 2011. Fundamentals of heat and mass transfer, 7th edition.

[3] Sundén, Bengt, and Raj M. Manglik. Plate heat exchangers: design, applications and performance. Vol. 11. Wit Press, 2007.

[4] Murshed, SM Sohel, and Manuel Matos Lopes, eds. Heat exchangers: design, experiment and simulation. BoD–Books on Demand, 2017.

[5] Murshed, SM Sohel, and Manuel Matos Lopes, eds. Heat Exchangers: Advanced Features and Applications. BoD–Books on Demand, 2017.

[6] ForumAutomation.com Available: https://forumautomation.com/t/what-is-heat-exchanger-applications-of-heat-exchangers/6143

[7] Nandi, S., et al. "Process identification using genetic programming, In “Petroleum Refining and petrochemical-based Industries in Eastern India,” Eds. RK Saha, S. Ray, BR Maity, D. Bhattacharya, S. Ganguly and S. L. Chakraborty." (2000): 195-201.

[8] Kenneth J. Bell, in Encyclopedia of Physical Science and Technology (Third Edition), 2003.

[9] JRC, DIRECTORATE-GENERAL. "Integrated Pollution Prevention and Control Draft Reference Document on Best Available Techniques in the Food, Drink and Milk Industry Final Draft June 2005."

[10] Prevention, Integrated Pollution. "Control Reference Document on Best Available Techniques in the Food, Drink and Milk Industries." European Commission, August (2006). Available: http://wetswegwijzer.nl/brefs/voedingsmiddelenenzuivel.pdf

[11] wiki.zero-emissions.at [Online] Available: http://wiki.zero-emissions.at/index.php?title=Pasteurization_in_food_industry

[12] Wikipedia: Types of Heat Exchangers, Finned Heat Exchangers, Overall heat transfer coefficient, Joule-Thomson Effect, Heat transfer in solar panels.

[13] Fatima Fazeli. Thermodynamics and Heat Transfer: Heat Exchangers. Montanüniversität Leoben, 2019.

[14] EngineeringToolBox.com [Online] Available: https://www.engineeringtoolbox.com/ansi-steel-pipes-d_305.html

[15] www.hyfoma.com [Online] Available: http://www.hyfoma.com/en/content/processing-technology/decontamination/

[16] Process-Heating.com [Online] Available: https://www.process-heating.com/articles/92458-process-applications-for-heat-exchangers

[17] Shah, R. K., B. Thonon, and D. M. Benforado. "Opportunities for heat exchanger applications in environmental systems." *Applied Thermal Engineering* 20.7 (2000)

[18] National Climate Change Secretariat and National Research Foundation. [Online] Available: https://www.nccs.gov.sg/docs/default-source/default-document-library/solar-energy-technology-primer-a-summary.pdf

[19] Energy.gov [Online] Available: https://www.energy.gov/energysaver/heat-exchangers-solar-water-heating-systems

[20] gea.com [Online] Available: https://www.gea.com/en/customer-cases/freeze-drying-fundamentals.jsp

[21] pharmaapproach.com [Online] Available: https://www.pharmapproach.com/manufacture-of-pharmaceutical-tablets/

[22] hrs-heatexchangers.com [Online] Available: https://www.hrs-heatexchangers.com/news/preventing-product-contamination-with-double-tube-plate-heat-exchangers/

[23] Helmut Weiss, Energy Efficiency in Petroleum Production, Leoben: Montanüniversität Leoben, 2017.

[24] Necati Ozisik, M., “Heat transfer: A basic approach”. New York: McGraw-Hill, 1985.

[25] Hardik V. Solanki, Jignesh M Barot. “CFD Analysis of Double Pipe Heat Exchanger with Twisted Tape Insert in Inner Pipe.”, 2018. [Online] Available: https://www.ijrti.org.

[26] Energy Transfer 2012 – 2020 [Online] Available: https://durafintube.com/fin-tube-surface-area-calculator/

[27] Engineers Edge 2000 – 2021 [Online] Available: www.engineersedge.com

[28] Jouhara, Hussam & Khordehgah, Navid & Almahmoud, Sulaiman & Delpech, Bertrand & Chauhan, Amisha & Tassou, Savvas. Waste Heat Recovery Technologies and Applications. Thermal Science and Engineering Progress, 2018.

[29] Robert A. Ackermann, “Regenerative Heat Exchanger Theory”, Cryogenic Regenerative Heat Exchangers, 1997.

List of Tables

Table 1: Pasteurization conditions [10] 12
Table 2: Physical properties of used fluids 18
Table 3: Summary of e-NTU VS OLGA results 48
Table 4: Summary of outlet temperature values for different conditions 53
Table 5: Summary of the difference in outlet temperature for two cases of comparison 54

List of Figures

Figure 1: Schematic of a shell-and -tube HX [24]..... 3
Figure 2: Schematic of a double-pipe HX [25] 4
Figure 3: Schematic of a finned-tube HX [26] 4
Figure 4: Schematic of parallel flow and counter flow arrangements [27] 6
Figure 5: Schematic of a crossflow arrangement [27] 6
Figure 6: Schematic of a plate HX [28] 5
Figure 7: Schematic of a regenerator HX [29]..... 7
Figure 8: Absorption/evaporation flowchart [3]..... 9
Figure 9: Petrochemical process of heating cryogenic fluids [7].....10
Figure 10: Basic design of a turbo-jet engine [5].....11
Figure 11: Configuration of a pasteurization HX [3] 13
Figure 12: Solar thermal domestic water heating system [18].....14
Figure 13: First step of fluid properties calculations 22
Figure 14: Temperature profile in a counter-flow HX [2].....23
Figure 15: Second step of fluid properties calculations 25
Figure 16: Setting the thermal properties of the fluids. 27
Figure 17: Reynolds number, Nusselt number and heat transfer coefficient calculation.....27
Figure 18: Heat transfer path and parameters in a double-pipe HX [1] 28
Figure 19: Resistivity and overall heat transfer coefficient calculations 30
Figure 20: HX surface area and length calculations.....31
Figure 21: Model Browser Lay-out.....33
Figure 22: Layout of the "Structural" folder 33
Figure 23: Layout of the "Case Definition" folder 34
Figure 24: Layout of the "Compositional" folder.....35
Figure 25: Layout of the "Flow Component" folder.....36
Figure 26: Layout of the "Flow Path" component for the cold fluid 37
Figure 27: Layout of the "Initial Conditions" sub-folder for the cold fluid.....38
Figure 28: Layout of the "Source" sub-folder for the cold fluid 39
Figure 29: Component Scheme.....39
Figure 30: Layout of the "Output" sub-folder for the cold fluid 40

Figure 31: Layout of the "Piping" sub-folder for the cold fluid 40
Figure 32: Layout of the "Positions" sub-folder for the cold fluid 41
Figure 33: Layout of the "Output" and "Thermal component" folders 42
Figure 34: Fluid bundle layout 43
Figure 35: Pipe arrangement of the HX at the testing facility 44
Figure 36: Variable guide of the e-NTU method 46
Figure 37: Comparing simulation results to e-NTU. 48
Figure 38: Summary of the results of the reverse-calculation method 49
Figure 39: Case 1 of simulation results 50
Figure 40: Case 2 of simulation results 50
Figure 41: Case 3 of simulation results 51
Figure 42: Case 4 of simulation results 51
Figure 43: Case 5 of simulation results 52
Figure 44: Case 6 of simulation results 52
Figure 45: Case 1 of e-NTU method results 53
Figure 46: Case 2 of e-NTU method results 53
Figure 47: Case 3 of e-NTU method results 53
Figure 48: Case 4 of e-NTU method results 54
Figure 49: Case 5 of e-NTU method results 54
Figure 50: Case 6 of e-NTU method results 54
Figure 51: Case 1 of insulated conditions 66
Figure 52: Case 2 of insulated conditions 66
Figure 53: Case 3 of insulated conditions 66
Figure 54: Case 4 of insulated conditions 67
Figure 55: Case 5 of insulated conditions 67
Figure 56: Case 6 of insulated conditions 67

Abbreviations

HX	Heat Exchanger
NTU	Number of Transfer Units
e-NTU	Effectiveness Number of Transfer Units
LMTD	Log Mean Temperature Difference
ESP	Electric Submersible Pump
VOC	Volatile Organic Component
HTST	High Temperature Short Time pasteurization
HHST	High Heat Short Time pasteurization

Nomenclature

ΔT_{lm}	Mean temperature difference [°C]
ΔT_1	Temperature difference at the inlet [°C]
ΔT_2	Temperature difference at the outlet [°C]
$T_{h,I}$	Inlet temperature of the hot fluid [°C]
$T_{h,o}$	Outlet temperature of the hot fluid [°C]
$T_{c,I}$	Inlet temperature of the cold fluid [°C]
$T_{c,o}$	Outer temperature of the cold fluid [°C]
$\dot{m}$	Mass flow rate [kg/s]
q_c	Flow rate of the cold fluid [m^3/h]
q_h	Flow rate of the hot fluid [m^3/h]
ρ_w	Density of water [kg/m^3]
C	Heat capacity rate [w/k]
c_p	Specific heat [J/kg.K]
C_{min}	Minimum heat capacity rate [w/k]
C_{max}	Maximum heat capacity rate [w/k]
$\dot{Q}$	Heat Transfer Rate [kW]
$\dot{Q}_{max}$	Maximum Heat Transfer Rate [kW]
ΔT_{max}	Maximum Temperature Difference [°C]
ε	Effectiveness [-]
c	Capacity ratio [-]
NTU	Number of Transfer Units [-]
A_s	Total surface area of heat transfer [m²]
V	Average velocity [m/s]
d_i	Inner pipe diameter [m]
d_o	Outer pipe diameter [m]
$d_{i,i}$	Inner diameter of the inner pipe [m]
$d_{i,o}$	Inner diameter of the outer pipe [m]
$d_{o,i}$	Outer diameter of the inner pipe [m]
$d_{o,o}$	Outer diameter of the outer pipe [m]
v	Kinematic viscosity [m²/s]
Re	Reynold's Number [-]
Nu	Nusselt Number [-]
Pr	Prandtl Number [-]
k	Thermal conductivity [W/m.K]
R_{total}	Total resistance of the system [°C/W]
R_{walll}	Wall resistance [°C/W]
R_i	Inner wall Resistance [°C/W]
R_o	Outer wall Resistance [°C/W]
A_i	Inner area of the inner pipe wall [m²]
A_o	Outer area of the inner pipe wall [m²]

L Pipe length [m]
U Overall heat transfer coefficient [W/m².K]
U_o Overall heat transfer coefficient for the cold fluid [W/m².K]
U_i Overall heat transfer coefficient for the hot fluid [W/m².K]
h Convective heat transfer coefficient [W/m².K]
h_o Convective heat transfer coefficient for the cold fluid [W/m².K]
h_i Convective heat transfer coefficient for the hot fluid [W/m².K]

Appendix

Results of the OLGA simulation under an insulated system

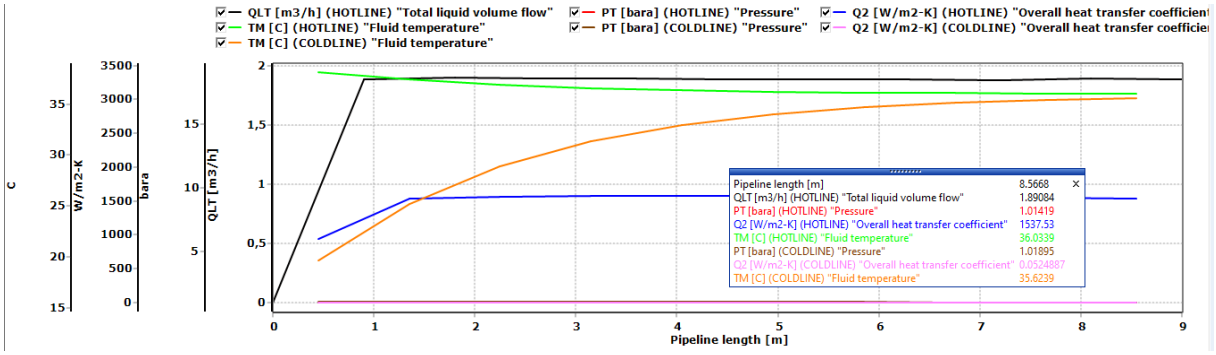

Figure 51: Case 1 of insulated conditions

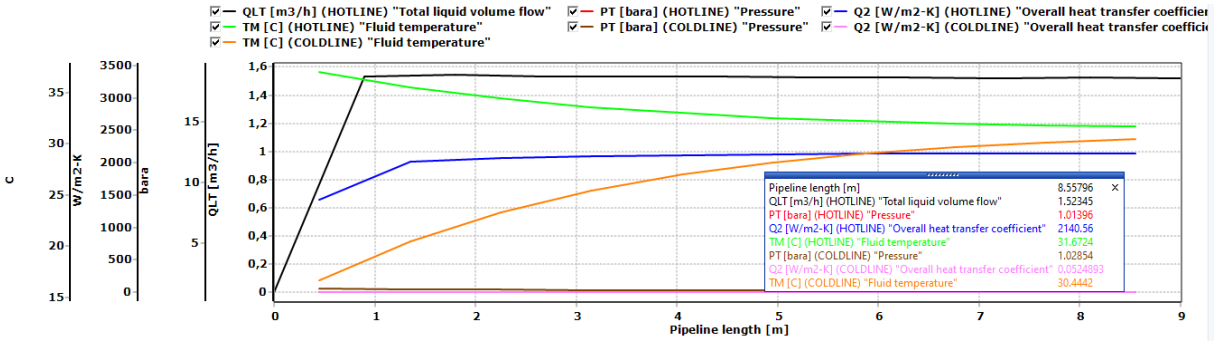

Figure 52: Case 2 of insulated conditions

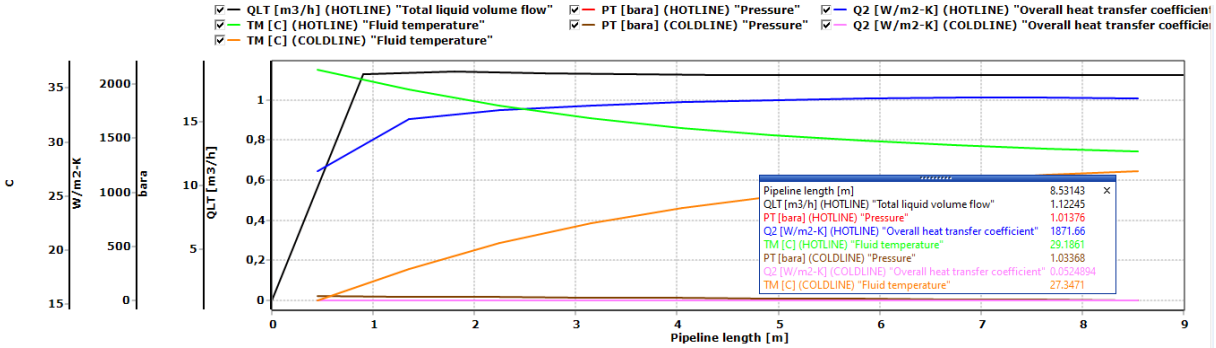

Figure 53: Case 3 of insulated conditions

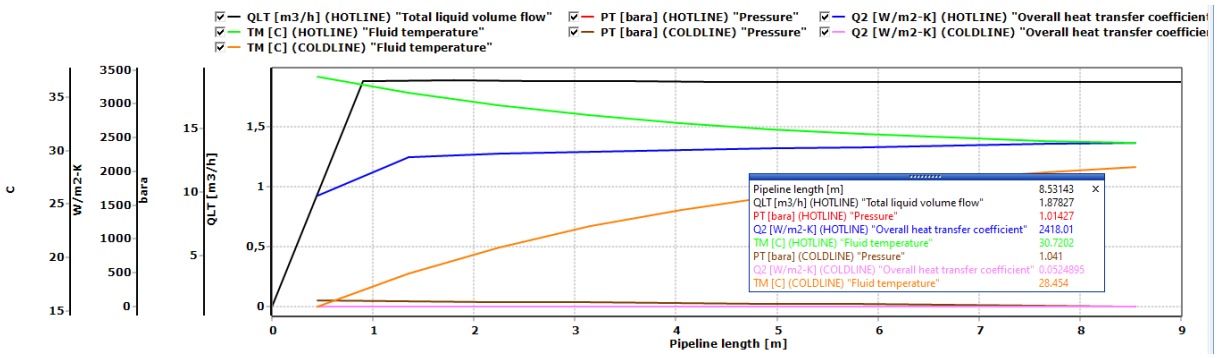

Figure 54: Case 4 of insulated conditions

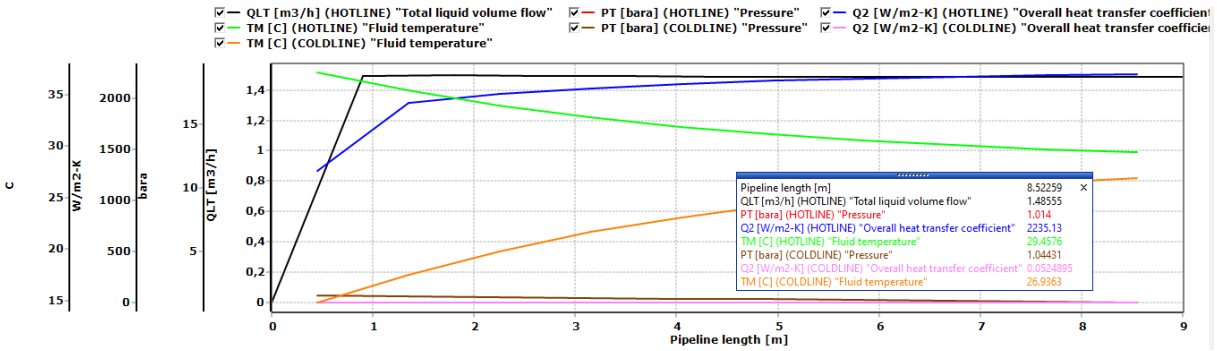

Figure 55: Case 5 of insulated conditions

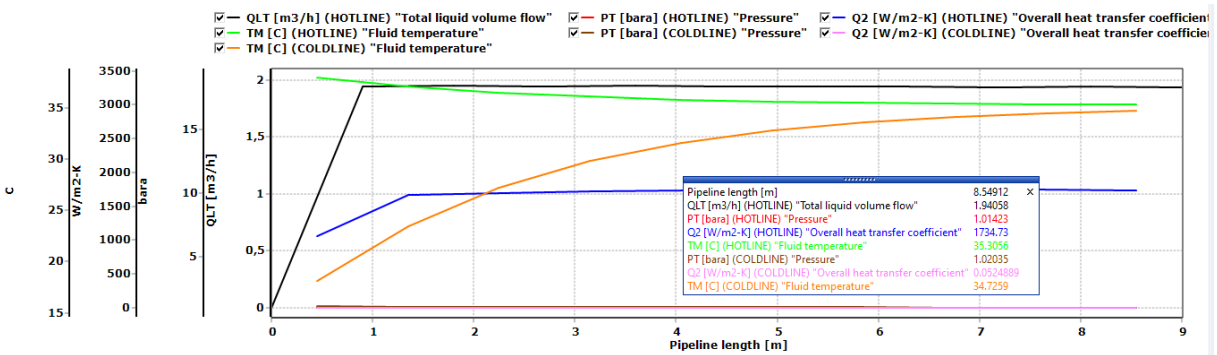

Figure 56: Case 6 of insulated conditions